Nuclear Tomography in UPC and at EIC

Measurement of e^+e^- Momentum and Angular Distributions from Linearly Polarized Photon Collisions

J. Adam *et al.* (STAR Collaboration)
Phys. Rev. Lett. **127**, 052302 – Published 27 July 2021

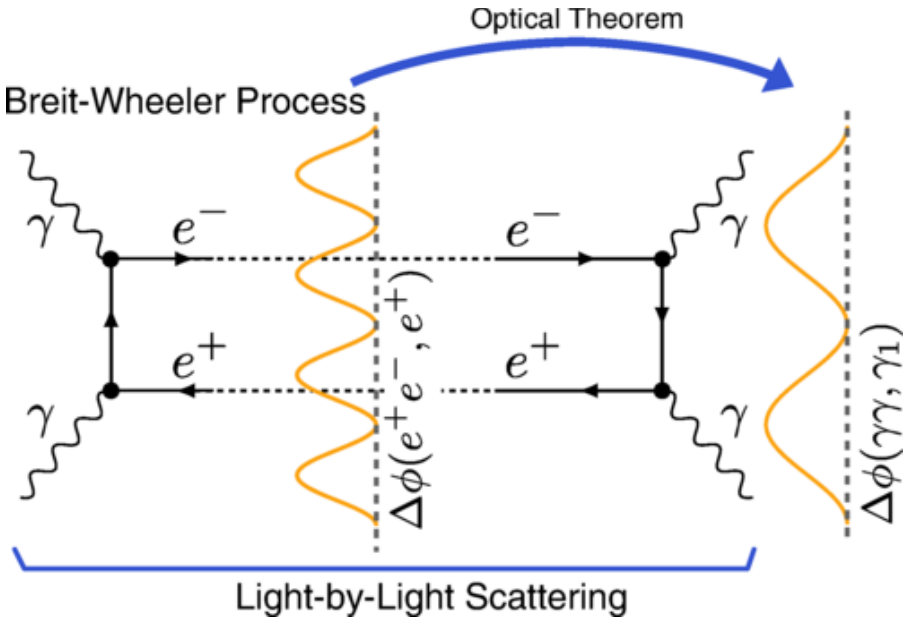

Zhangbu Xu

(Kent State University & BNL)

- Basic pure EM and Diffractive processes in Heavy-ion collisions
- charge radii of ^{197}Au/^{238}U at RHIC
- mass radii at RHIC
- Projective Imaging of nuclear geometry at EIC
- What defines COHERENT Diffractive?
- Summary

Two-photon QED in Particle Data Book

51.7 Two-photon processes

In the Weizsäcker-Williams picture, a high-energy electron beam is accompanied by a spectrum of virtual photons of energies ω and invariant-mass squared $q^2 = -Q^2$, for which the photon number density is

$$dn = \frac{\alpha}{\pi}\left[1 - \frac{\omega}{E} + \frac{\omega^2}{E^2} - \frac{m_e^2\,\omega^2}{Q^2 E^2}\right]\frac{d\omega}{\omega}\frac{dQ^2}{Q^2}, \tag{51.43}$$

where E is the energy of the electron beam. The cross section for $e^+e^- \to e^+e^-X$ is then [9]

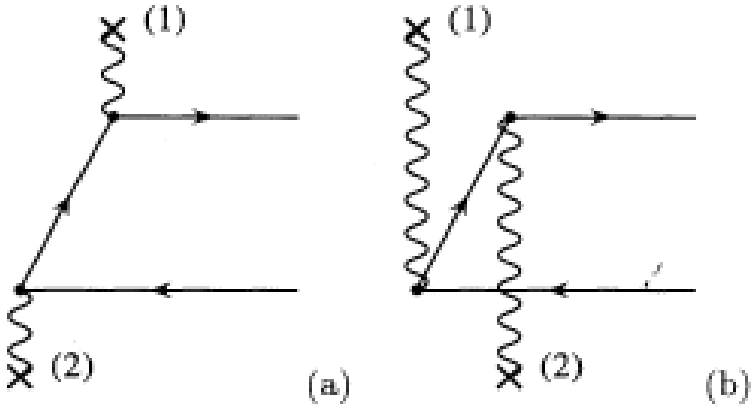

$$d\sigma_{e^+e^-\to e^+e^-X}(s) = dn_1\, dn_2\, d\sigma_{\gamma\gamma\to X}(W^2), \tag{51.44}$$

Two cutoffs:

ω<E

Q>0

Natural extension to Heavy Ions

$$\rho_A(r) = \frac{\rho^0}{1 + \exp[(r - R_{\rm WS})/d]}$$

$$dn_i = \frac{Z_i^2 \alpha}{\pi^2} \frac{q_{i\perp}^2 \left[F\left(q_{i\perp}^2 + \frac{w_i^2}{\gamma^2}\right)\right]^2}{\left(q_{i\perp}^2 + \frac{w_i^2}{\gamma^2}\right)^2} \frac{d^3 q_i}{w_i} \qquad (1)$$

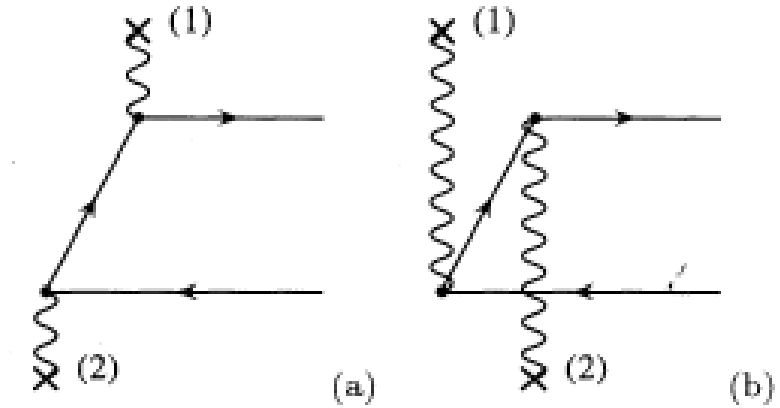

$$\sigma = 16 \frac{Z^4 e^4}{(4\pi)^2} \int \frac{dw_1}{w_1} \frac{dw_2}{w_2} \frac{d^2 k_{1\perp}}{(2\pi)^2} \frac{d^2 k_{2\perp}}{(2\pi)^2} \left| \frac{F(-k_1^2)}{k_1^2} \right|^2 \times \left| \frac{F(-k_2^2)}{k_2^2} \right|^2 k_{1\perp}^2 k_{2\perp}^2 \sigma(w_1, w_2) \qquad (6)$$

arXiv:1005.3531, unpublished

S. Klein, et al. Comput.Phys.Commun. 212 (2017) 258-268

Initial Transverse Momentum Broadening

$$\sigma = 16\frac{Z^4e^4}{(4\pi)^2}\int d^2b\int \frac{dw_1}{w_1}\frac{dw_2}{w_2}\frac{d^2k_{1\perp}}{(2\pi)^2}\frac{d^2k_{2\perp}}{(2\pi)^2}\frac{d^2q_\perp}{(2\pi)^2}$$
$$\times \frac{F(-k_1^2)}{k_1^2}\frac{F(-k_2^2)}{k_2^2}\frac{F^*(-k_1'^2)}{k_1'^2}\frac{F^*(-k_2'^2)}{k_2'^2}e^{-i\vec{b}\cdot\vec{q}_\perp} \qquad (2)$$
$$\times \left[(\vec{k}_{1\perp}\cdot\vec{k}_{2\perp})(\vec{k}'_{1\perp}\cdot\vec{k}'_{2\perp})\sigma_s(w_1,w_2)\right.$$
$$\left.+(\vec{k}_{1\perp}\times\vec{k}_{2\perp})(\vec{k}'_{1\perp}\times\vec{k}'_{2\perp})\sigma_{ps}(w_1,w_2)\right]$$

Zha, et al., arXiv: 1812.02820
M. Vidovic, et al., Phys.Rev. C47 (1993) 2308

$$\rho_A(r) = \frac{\rho^0}{1+\exp[(r-R_{\rm WS})/d]}$$

$$dn_i = \frac{Z_i^2\alpha}{\pi^2}\frac{q_{i\perp}^2\left[F\left(q_{i\perp}^2+\frac{w_i^2}{\gamma^2}\right)\right]^2}{\left(q_{i\perp}^2+\frac{w_i^2}{\gamma^2}\right)^2}\frac{d^3q_i}{w_i} \qquad (1)$$

arXiv:1005.3531, unpublished

$$\frac{d^2N_{\gamma\gamma}(k_1,k_2)}{dk_1dk_2} =$$
$$\int\int d^2b_1d^2b_2^2P_{\rm NOHAD}(|\vec{b_1}-\vec{b_2}|)N(k_1,\vec{b}_1)N(k_2,\vec{b}_2) \qquad (4)$$

S. Klein, et al. Comput.Phys.Commun. 212 (2017) 258-268

Is photon pt really driven by uncertainty principle and independent of position-momentum correlation?

we can afford many mistakes in the search. The main thing is to make them as fast as possible.
– John Archibald Wheeler
doi:10.1063/1.3120895

$\omega/\gamma \lesssim kt << \omega$
Higher-order/virtuality cancels to $1/\gamma^2 \sim = 10^{-4}$
NLO QED coupling constant $\alpha = 1/137$

Ultra-Peripheral Collisions

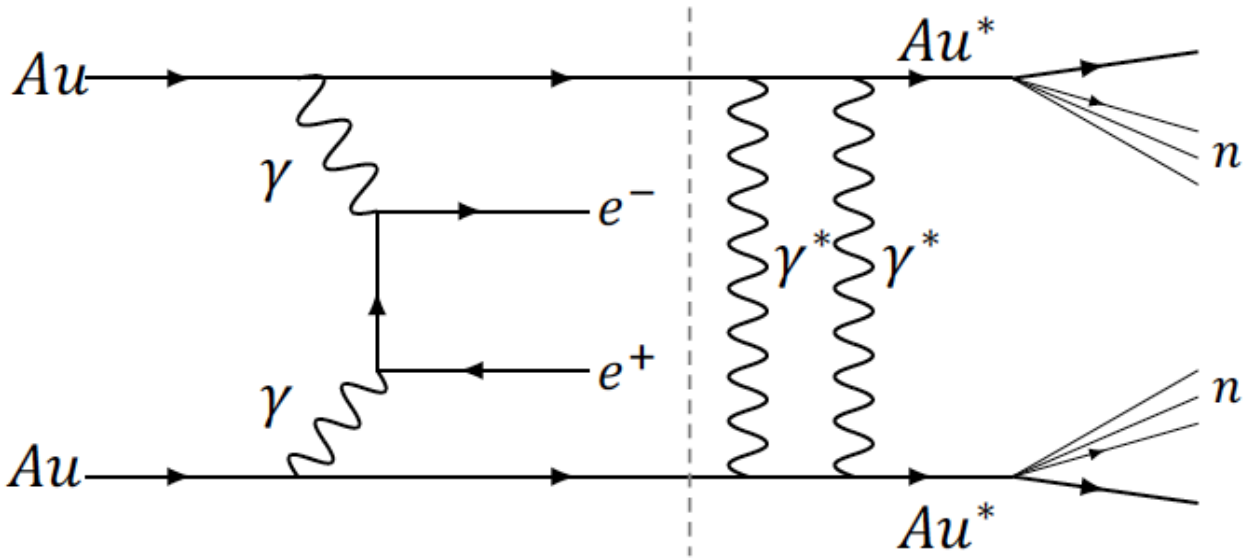

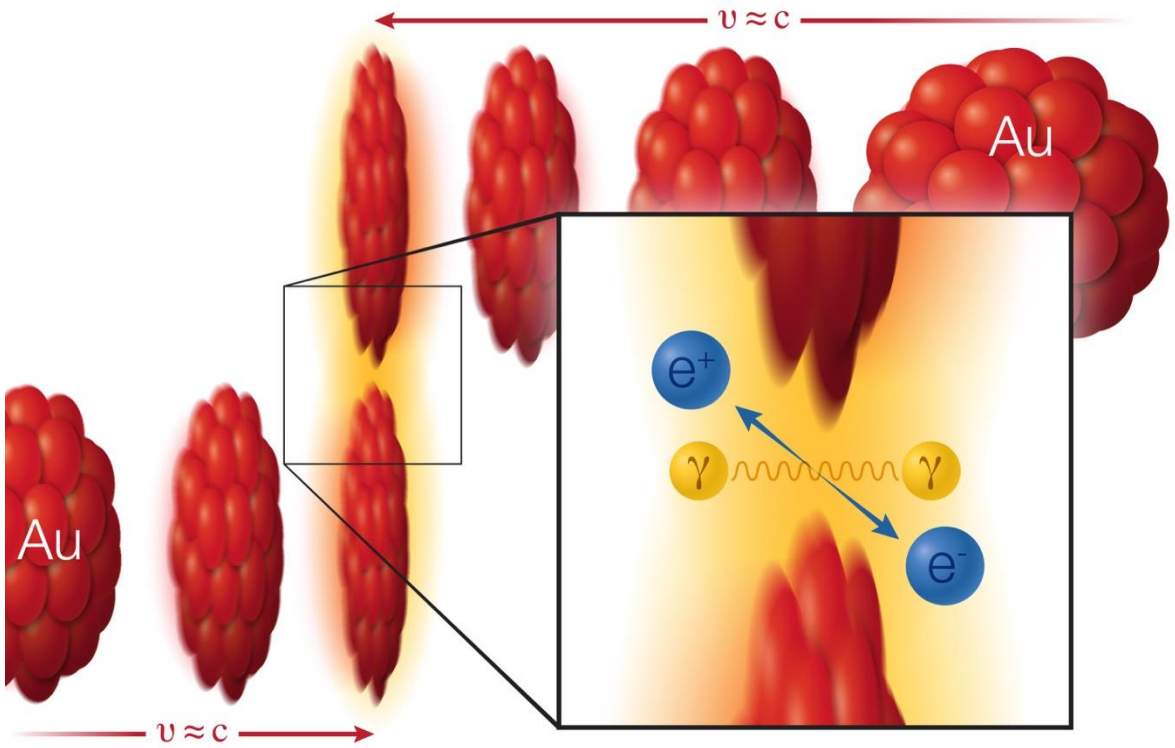

Two gold (Au) ions (red) move in opposite direction at 99.995% of the speed of light (v, for velocity, = approximately c, the speed of light). As the ions pass one another without colliding, two photons (γ) from the electromagnetic cloud surrounding the ions can interact with each other to create a matter-antimatter pair: an electron (e^-) and positron (e^+).

Well understood kinematics

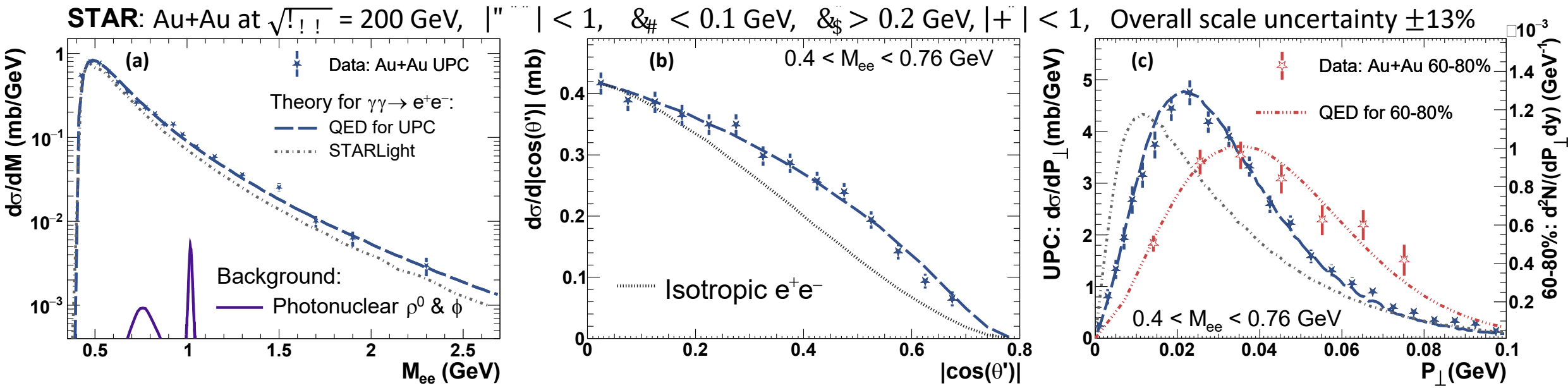

ρ,ϕ,ω<±0.2%

<±2%

<±2%

photon p_T is simply due to finite electric field projection in the longitudinal direction,
It is classic EM field and not due to uncertainty principle of p_T~=1/R

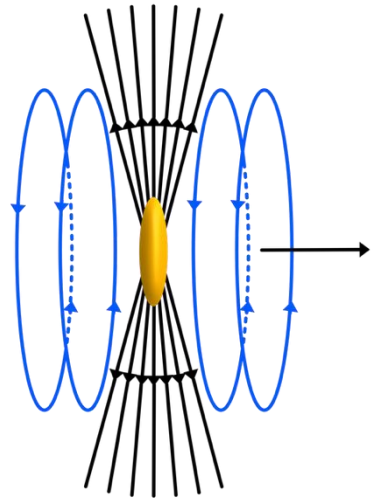

E field has a z-component
B field is in x-y plane
➔
ExB has p_T component
10—20MeV in p_T
Acting on the nucleus as a whole

Photon TMD in UPC

CMS Abstract: "This observation demonstrates the transverse momentum and energy of photons emitted from relativistic ions have impact parameter dependence. These results constrain precision modeling of initial photon-induced interactions in ultra-peripheral collisions. They also provide a controllable baseline to search for possible final-state effects on lepton pairs resulting from the production of quark-gluon plasma in hadronic heavy ion collisions."

https://news.rice.edu/2021/09/20/physicists-probe-light-smashups-to-guide-future-research-2/

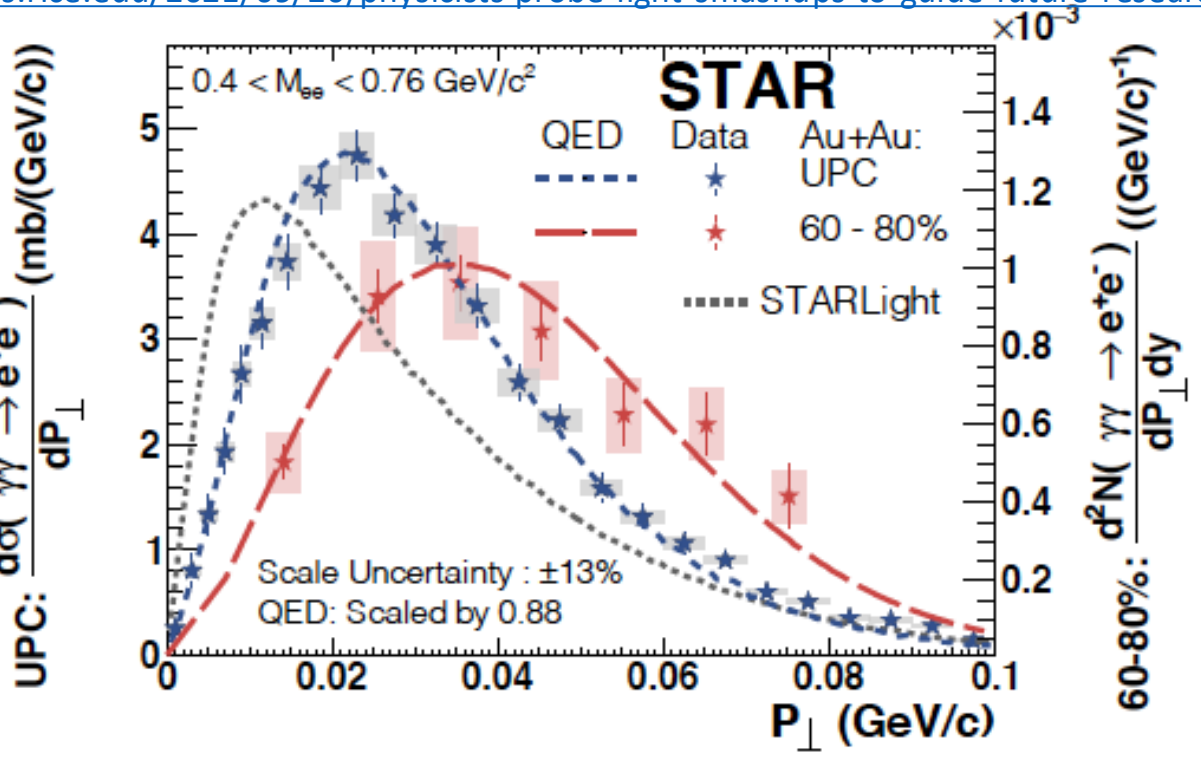

50. STAR Collaboration, J., Adam *et al.* Probing Extreme Electromagnetic Fields with the Breit-Wheeler Process. (2019). https://arxiv.org/abs/1910.12400.

51. ATLAS Collaboration. Measurement of non-exclusive dimuon pairs produced via $\gamma\gamma$ scattering in Pb+Pb collisions at $\sqrt{s_{NN}} = 5.02$ TeV with the ATLAS detector. ATLAS-CONF-2019-051. (2019). https://inspirehep.net/literature/1762955.

52. CMS Collaboration,. Observation of forward neutron multiplicity dependence of dimuon acoplanarity in ultra-peripheral PbPb collisions at $\sqrt{s_{NN}} = 5.02$ TeV CMS-PAS-HIN-19-014. (2020). https://inspirehep.net/literature/1798862.

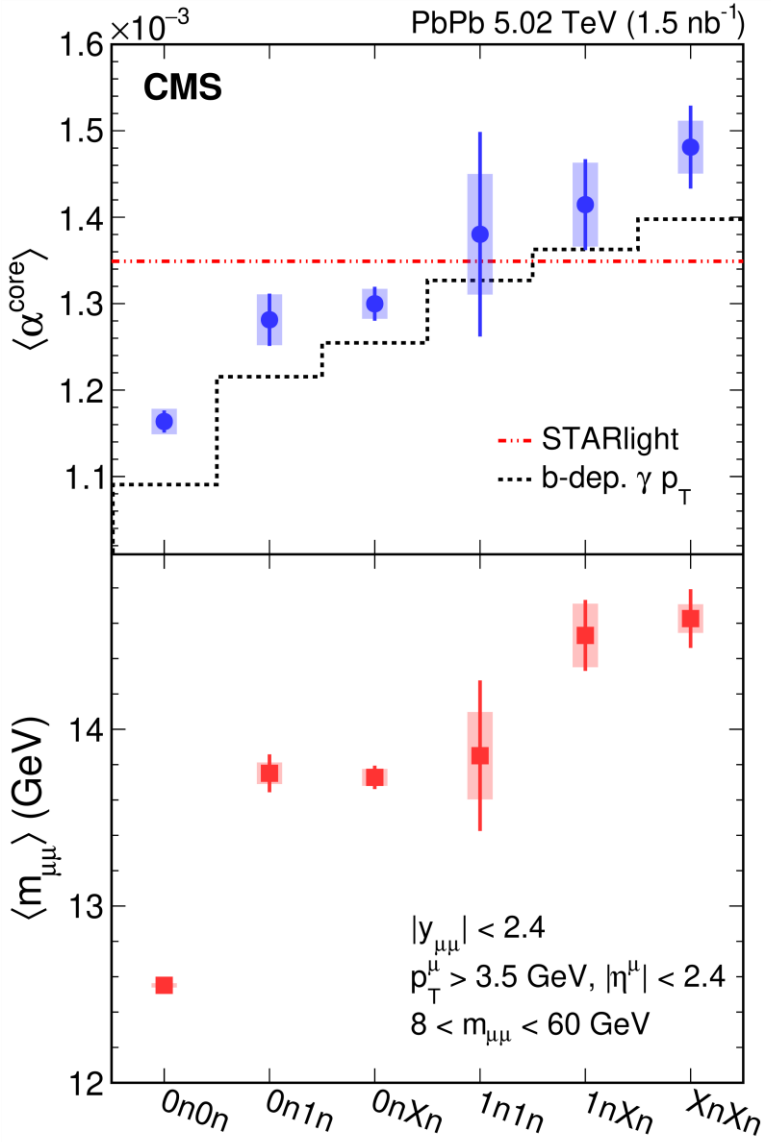

Criteria of a Breit-Wheeler process

be interpreted as a transition current,

$$J_{\mu\nu}(k_1k_2;P\alpha) = \Gamma_{\mu\nu}(k_1k_2;\alpha)\,(2\pi)^4\delta^4(k_1+k_2-P) \quad , \tag{7}$$

so that the S-matrix element (4) may be written as

$$S(P\alpha,\mathbf{b}) = \int \frac{d^4k_1}{(2\pi)^4} \int \frac{d^4k_2}{(2\pi)^4}\, A_1^\mu(k_1,\mathbf{b})\, A_2^\nu(k_2,0) \times J_{\mu\nu}(k_1k_2;P\alpha)\,. \tag{8}$$

The transition current is conserved, i.e.,

$$k_1^\mu J_{\mu\nu} = k_2^\nu J_{\mu\nu} = 0 \quad , \tag{9}$$

which follows quite generally from the gauge invariance of the S-matrix element.

For our following considerations the explicit expression for the transition current is irrelevant; it is only important that it acts like a conserved current (9) and contains a δ function (7) for the four-momentum conservation.

Performing the integrals over the δ functions, Eq. (8) becomes, with $Z_1 = Z_2 = Z$ and $F_1 = F_2 = F$,

$$S(P\alpha;\mathbf{b}) = Z^2\frac{e^2}{2\gamma^2}\int \frac{d^2k_\perp}{(2\pi)^2}\,\frac{F(-k_1^2)}{-k_1^2}\,\frac{F(-k_2^2)}{-k_2^2} \times u_{1\mu}u_{2\nu}\Gamma^{\mu\nu}(k_1k_2;\alpha)\,e^{-i\mathbf{b}\cdot\mathbf{k}_\perp}, \tag{10}$$

Vidovic *et al.*, PRC 1993

The nuclei move on straight trajectories and thus $k_z/k^0 = \pm 1/v$, confer Eq. (11). We obtain

$$u_{1\mu}u_{2\nu}J^{\mu\nu} = \gamma^2\frac{k_{1i}}{k_{10}}\frac{k_{2j}}{k_{20}}J^{ij} + \frac{1}{v}\left(\frac{k_{2j}}{k_{20}}J^{3j} - \frac{k_{1i}}{k_{10}}J^{i3}\right) - \frac{1}{\gamma^2v^2}J^{33} \quad . \tag{25}$$

Precisely at this point we introduce the decisive approximations, which will lead to the equivalent photon result. The term ω/γ, which corresponds to k_0/γ or k_3/γ, is of the same order of magnitude as the term $|\mathbf{k}_\perp|$, which corresponds to k_i:

$$|\mathbf{k}_\perp| \approx \frac{1}{\gamma}|\mathbf{k}_\parallel| \approx \frac{\omega}{\gamma} \quad . \tag{26}$$

This can be verified by considering those values of $|\mathbf{k}_\perp|$, which contribute most in the integrand of the equivalent photon distribution (2). The same relation also holds, if one compares the transverse component of the Poynting vector to its longitudinal one.

For the scalar boson the dominant contribution in Eq. (25) originates from the first term; the second and third terms are suppressed by a factor of $1/\gamma^2$ with respect to the first one. The situation for the pseudoscalar boson (6), the charged boson pair, and the fermion pair is exactly the same.

$$u_{1\mu}u_{2\nu}\Gamma^{\mu\nu}(k_1k_2;\alpha) \approx \gamma^2\frac{k_{1i}}{\omega_1}\frac{k_{2j}}{\omega_2}\Gamma^{ij}(\omega_1\omega_2;\alpha). \tag{28}$$

On the right-hand side now appears the vertex function for real photons as in (19). This identification is the heart of the equivalent photon approach.

To qualify as a Breit-Wheeler process from Coulomb field:

$$\omega/\gamma \lesssim k_\perp \lesssim 1/R \ll \omega$$

X.F. Wang *et al.*, PRC 2023

Energy Dependence of Cross Section and $\sqrt{\langle p_T^2 \rangle}$

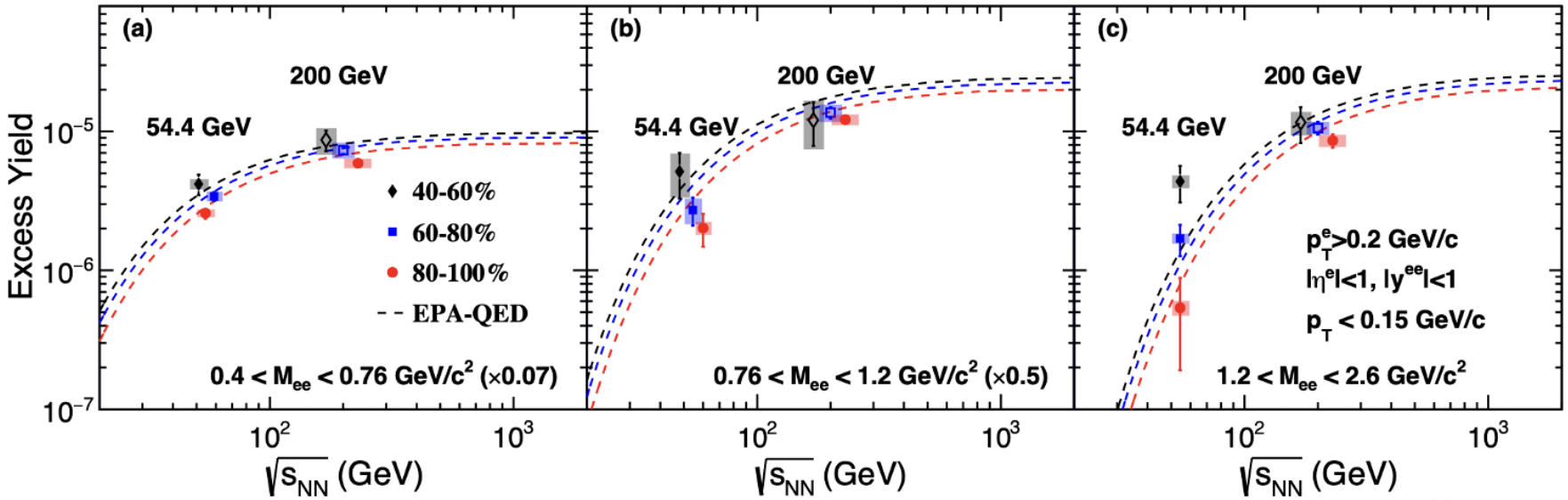

The kinematics of the Breit-Wheeler process are **sensitive** to the details of the **nuclear charge distribution**

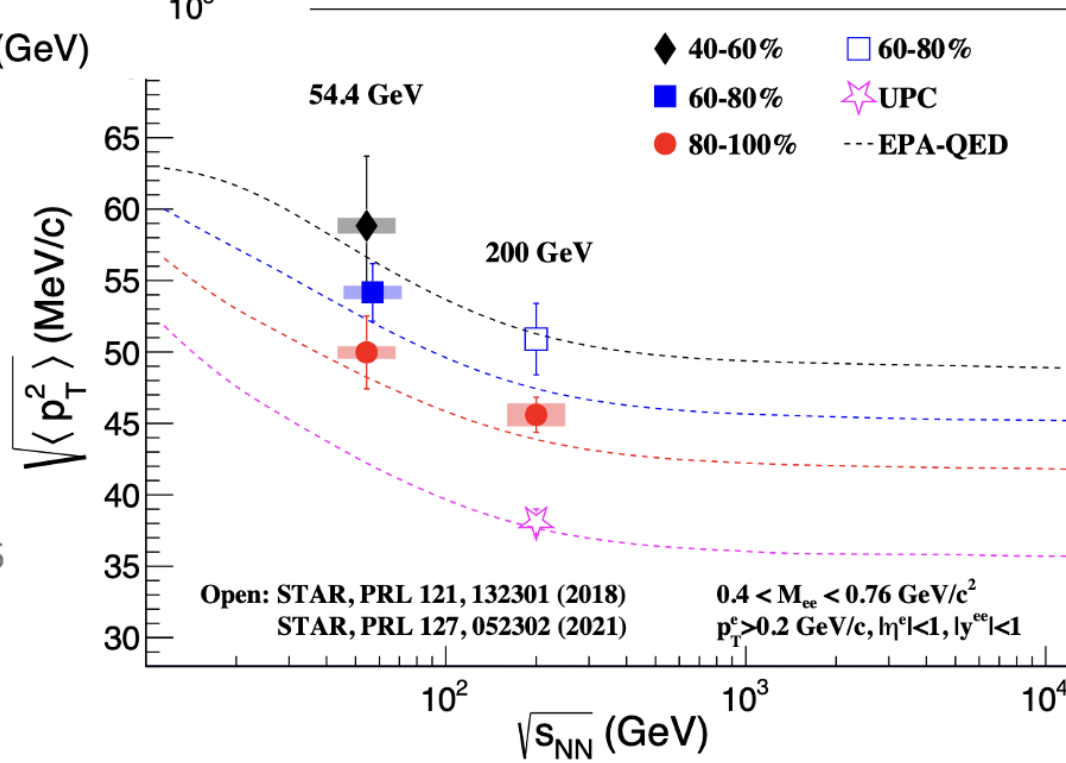

STAR Collaboration, Phys. Rev. C 111 (2025) 14909

X. W, J.D. Brandenburg, L. Ruan, F. Shao, Z. Xu, C. Yang, and W. Zha. Phys. Rev. C 107, 044906

Application: Mapping the Magnetic Field

Xiaofeng Wang@Scharff-Goldhaber Prize Ceremony
08/15/23

R. D. Woods and D. S. Saxon, Phys. Rev. 95, 577–578 (1954)

Woods-Saxon: $$\rho_A(r) = \frac{\rho^0}{1 + \exp[(r - R)/d]}$$

R: charge radius, d: skin depth

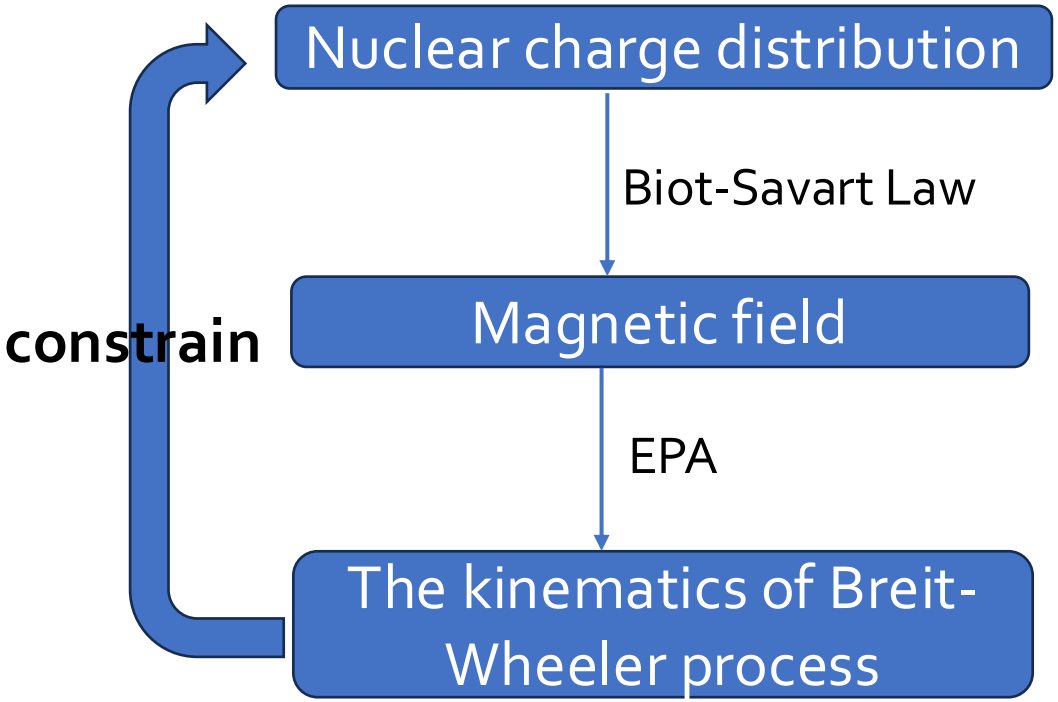

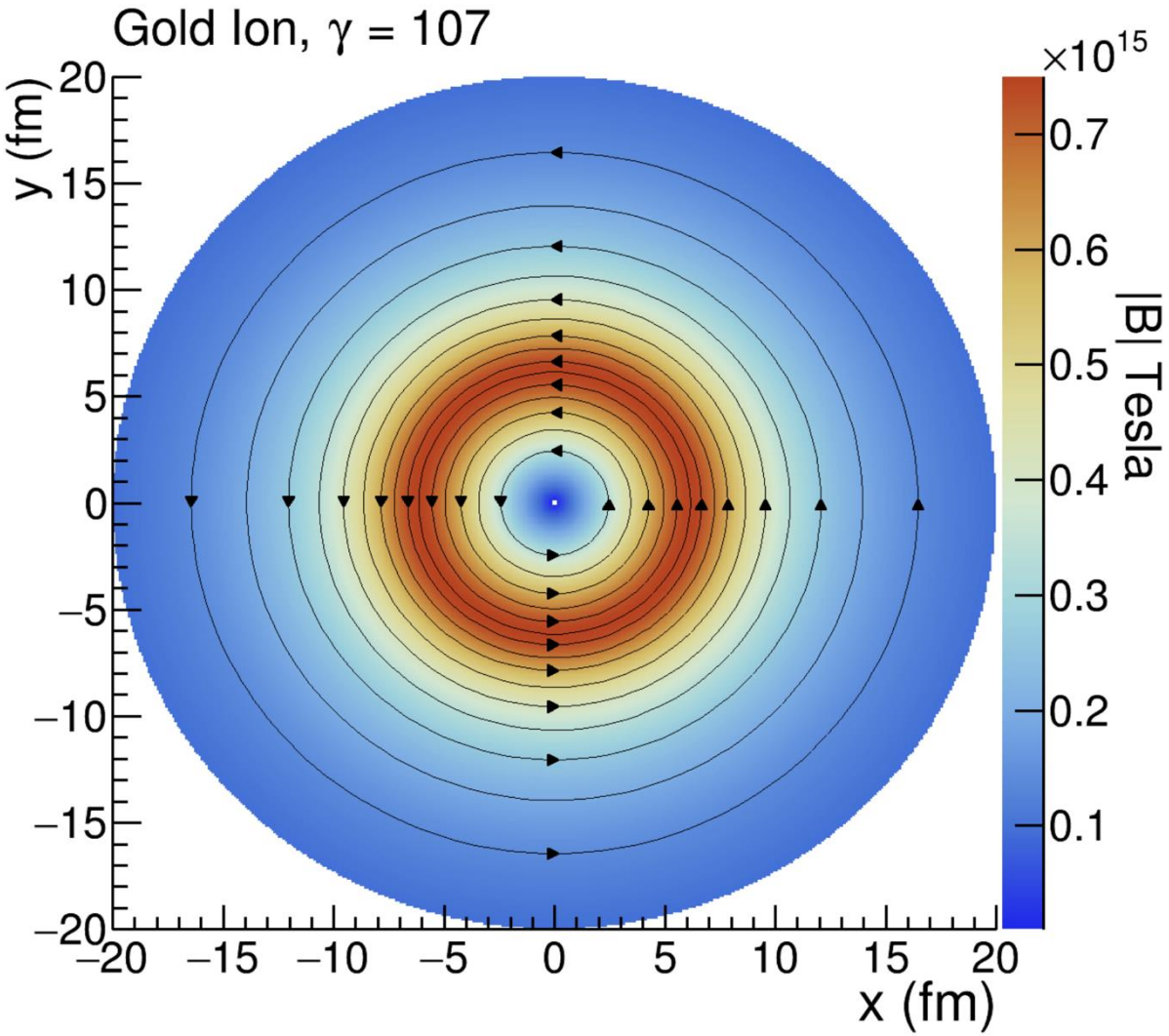

Constraint on charge distribution with precision

Using LO QED to calculate Breit-Wheeler process to match data with least-chi2

UPC consistent with nominal nuclear geometry

Peripheral collisions systematically larger

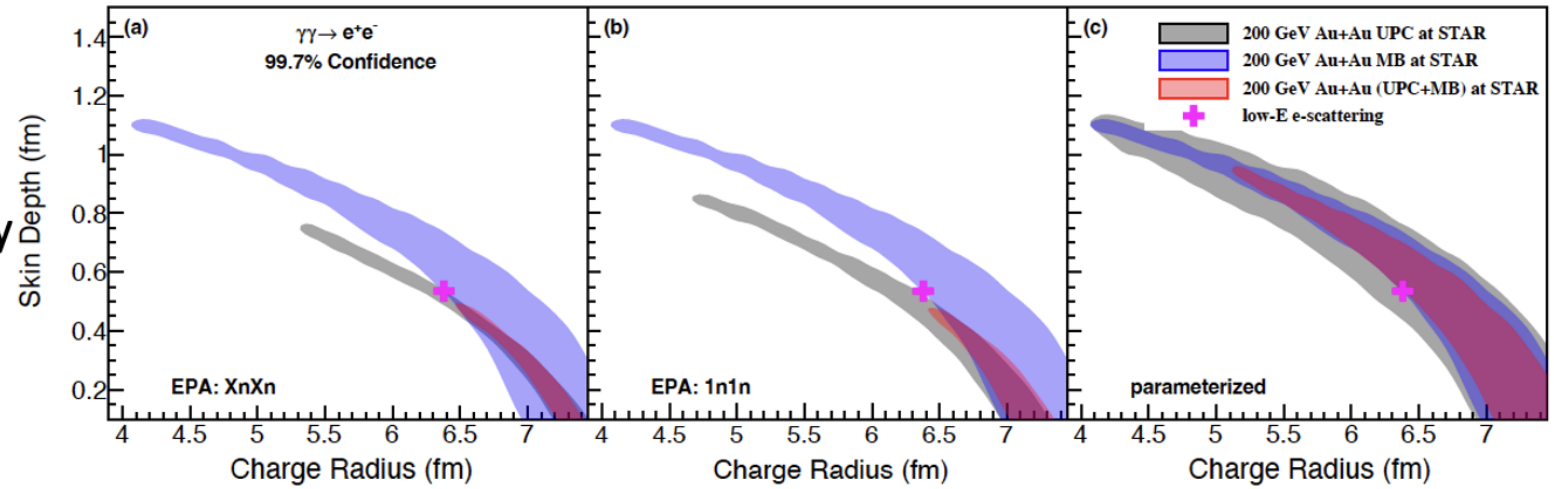

STAR Collaboration, **Phys. Rev. C 111** (2025) 14909
X. W, J.D. Brandenburg, L. Ruan, F. Shao, Z. Xu, C. Yang, and W. Zha. Phys. Rev. C 107, 044906 (2023)

TABLE I. RMS of radius ($\sqrt{\langle r^2 \rangle}$) at minimum χ^2 (χ^2_{min}) and uncertainties within $\chi^2_{min}+1$ with different σ_{NN} and with different neutron selection conditions in ZDC and parameterized probability. A default $\sigma_{NN} = 41.6$ mb has been used in all other calculations. These are to be compared to the default value of nuclear charge radius RMS of $\sqrt{\langle r^2 \rangle} = 5.33$ fm at $R = 6.38$ fm and $d = 0.535$ fm.

condition	σ_{NN} (mb)	UPC	MB	UPC+MB
1n1n	35.0	5.55 + 0.03 - 0.30	5.66 + 0.09 - 0.12	5.55 + 0.03 - 0.03
	40.0	5.32 + 0.26 - 0.21	5.67 + 0.08 - 0.10	5.58 + 0.01 - 0.04
	41.6	5.39 + 0.14 - 0.21	5.67 + 0.08 - 0.12	5.53 + 0.10 - 0.02
	45.0	5.47 + 0.02 - 0.21	5.66 + 0.09 - 0.11	5.54 + 0.08 - 0.03
XnXn	35.0	5.70 + 0.01 - 0.29	5.66 + 0.09 - 0.12	5.64 + 0.07 - 0.07
	40.0	5.70 + 0.01 - 0.30	5.67 + 0.08 - 0.10	5.70 + 0.01 - 0.12
	41.6	5.67 + 0.03 - 0.17	5.67 + 0.08 - 0.12	5.67 + 0.03 - 0.09
	45.0	5.54 + 0.17 - 0.16	5.66 + 0.09 - 0.11	5.64 + 0.06 - 0.11
Parameterized	35.0	5.51 + 0.15 - 0.18	5.66 + 0.09 - 0.12	5.61 + 0.13 - 0.11
	40.0	5.43 + 0.22 - 0.08	5.67 + 0.08 - 0.10	5.67 + 0.04 - 0.16
	41.6	5.41 + 0.25 - 0.09	5.67 + 0.08 - 0.12	5.62 + 0.12 - 0.11
	45.0	5.40 + 0.23 - 0.17	5.66 + 0.09 - 0.11	5.62 + 0.09 - 0.11

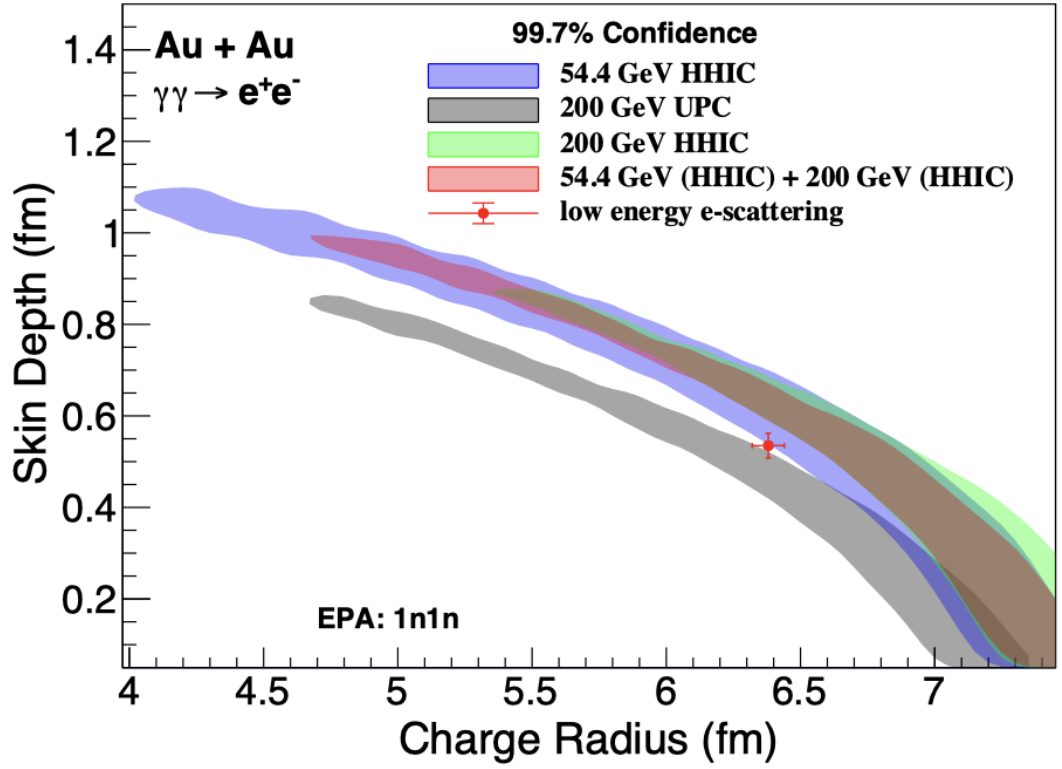

Imaging the nucleus with high-energy photons

Long history with some puzzling mysteries (20+ years):

Diffractive |t| pattern qualitatively resembles what it should be

Extracted radius is way too large (+1fm)

Cross sections are used for comparison to theory

Photon energy is 50-100GeV in the target frame

Klein and Mantysaari, Nature Reviews Physics 1 (2019) 662

ALICE, JHEP06 (2020) 35

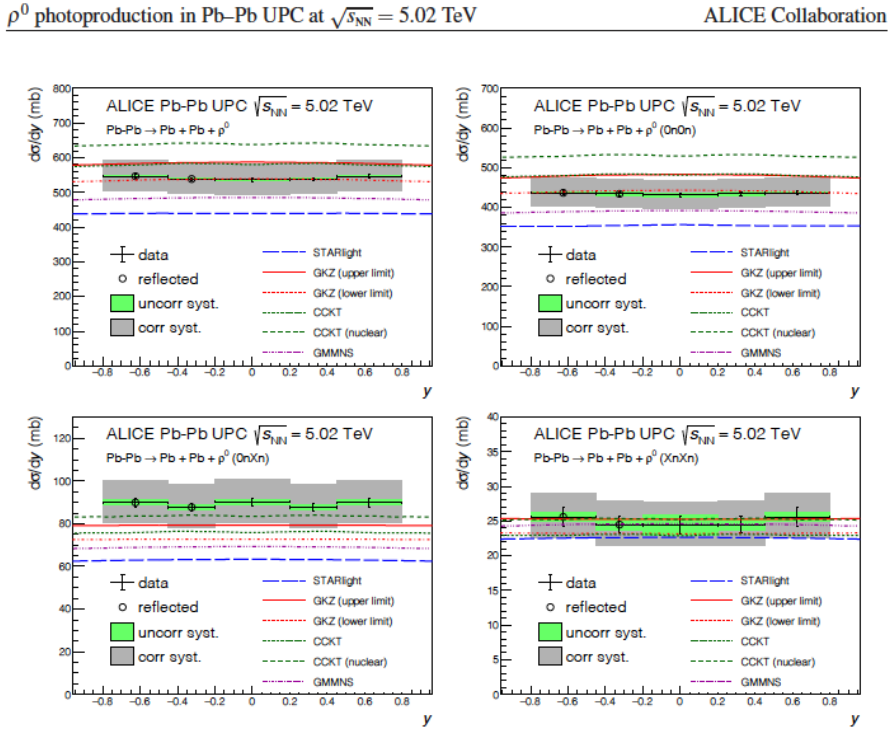

Figure 5: (Colour online). Cross section for the coherent photoproduction of ρ^0 vector mesons in Pb–Pb UPC as a function of rapidity for no forward-neutron selection (top left), and for the 0n0n (top right), 0nXn (bottom left) and XnXn (bottom right) classes. The lines show the predictions of the different models described in the text.

STAR, PRC 96 (2017) 54904

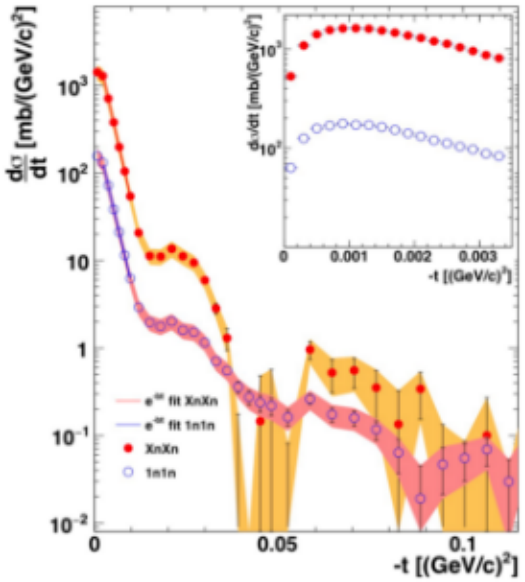

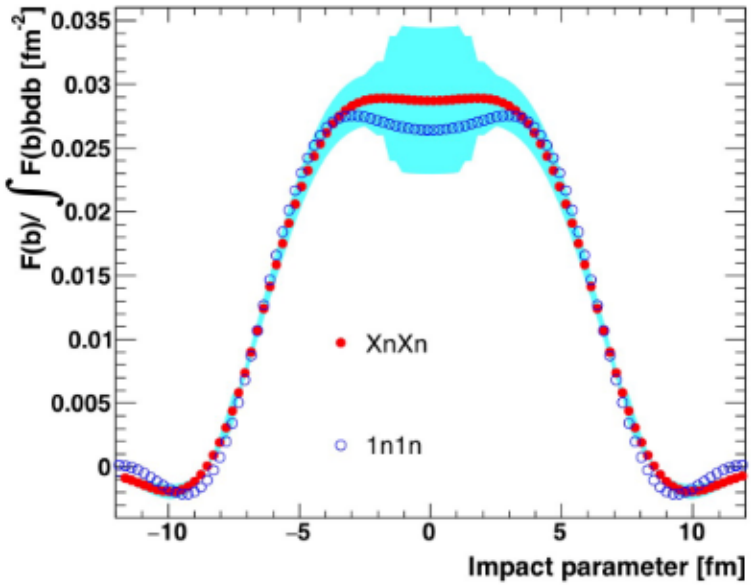

Left: The cross-section as a function of t, the squared momentum transfer to the nucleus. The dips and peaks are a diffraction pattern, akin to the pattern made by a 2-slit interferometer. 'XnXn' and '1n1n' are two different STAR data samples.The inset shows the distribution for very small momentum transfers. **Right:** The two-dimensional Fourier transform of the left panel, showing the density of the interaction sites in the nucleus, as a function of transverse distance from its center. This is a map of where the mesons interacted in the target. Although there is considerable systematic uncertainty (the blue region) near the center of the target, the edges of the nuclei are well defined.

Spin Interference Enabled Nuclear Tomography

STAR, arXiv:2204.01625

- Teaser:
  Polarized photon-gluon fusion reveals quantum wave interference of non-identical particles and shape of high-energy nuclei

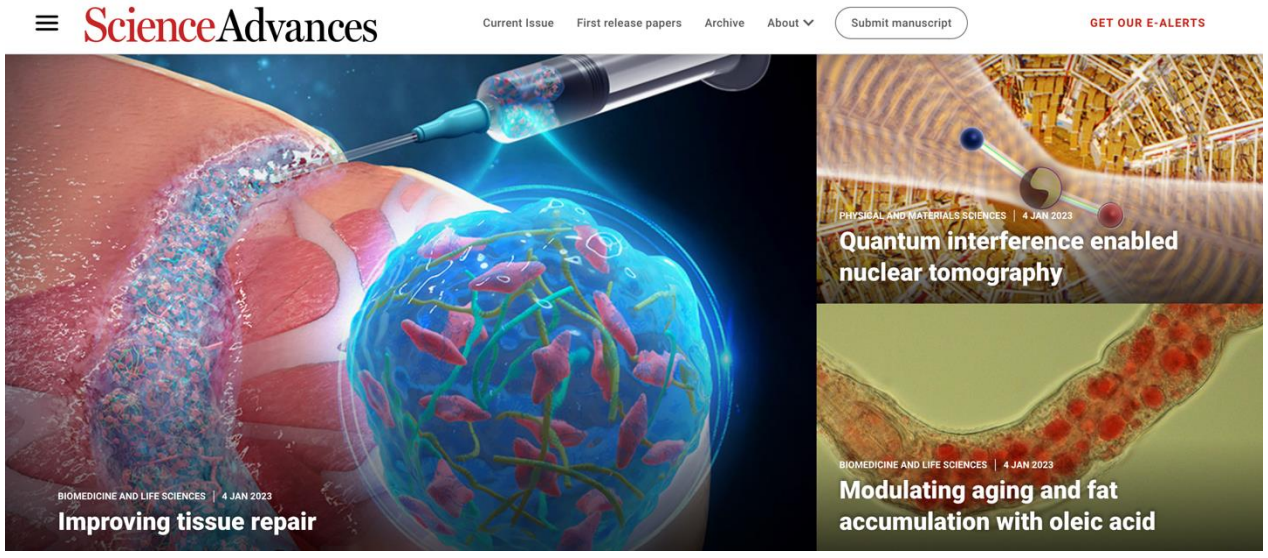

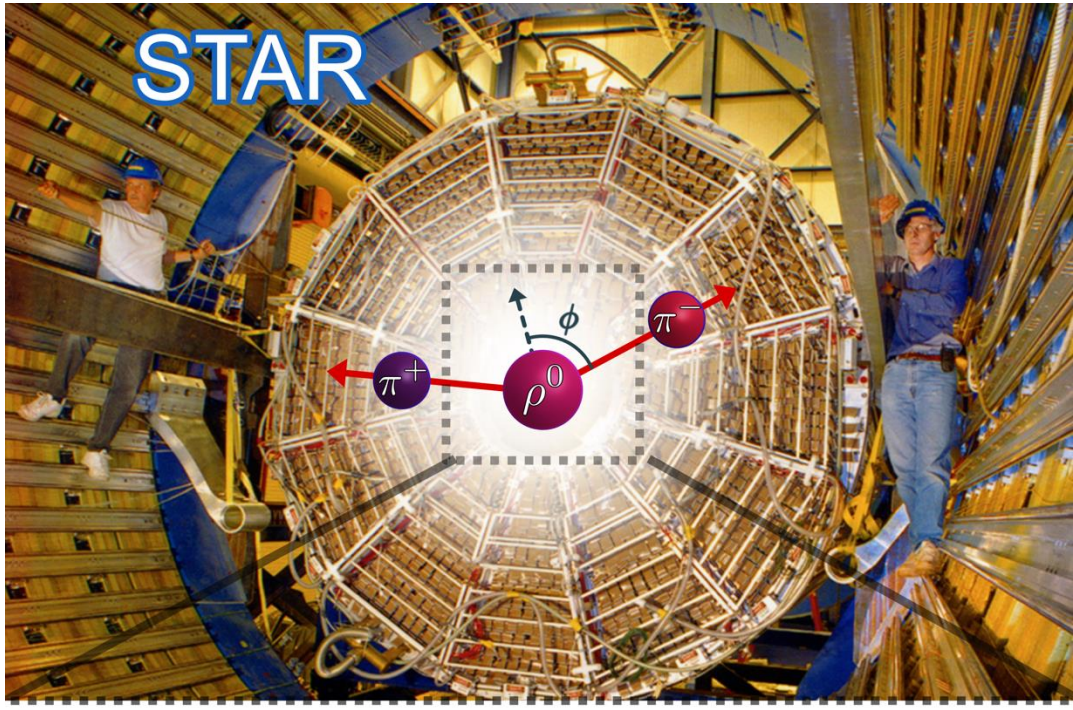

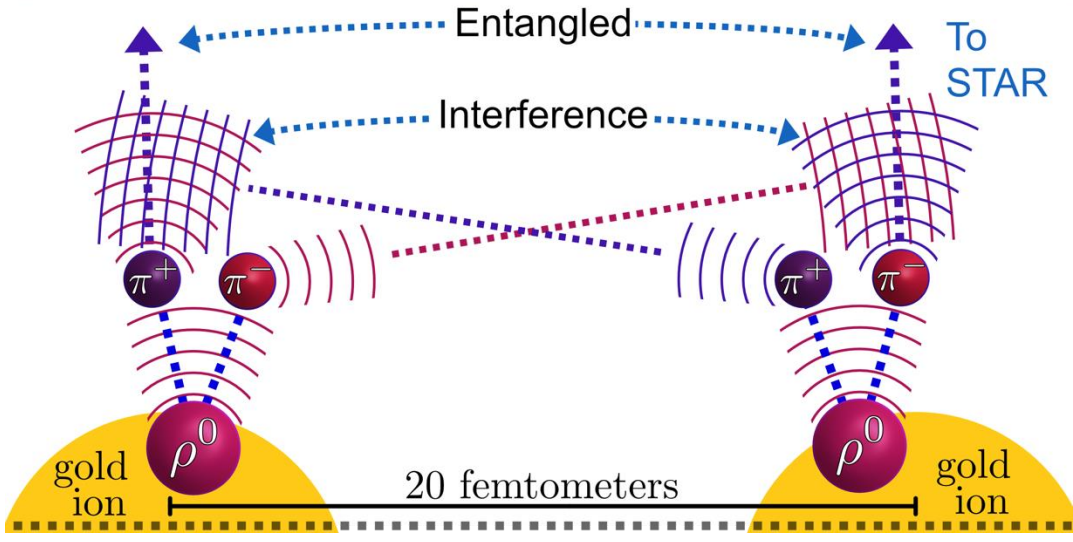

Three Ingredients

- Linearly Polarized photoproduction of vector meson
- At a distance with two wavefunctions (180° rotation symmetry)
- Entanglement between $\pi^{\pm}$ from ρ decay and interference between identical pion wavefunction

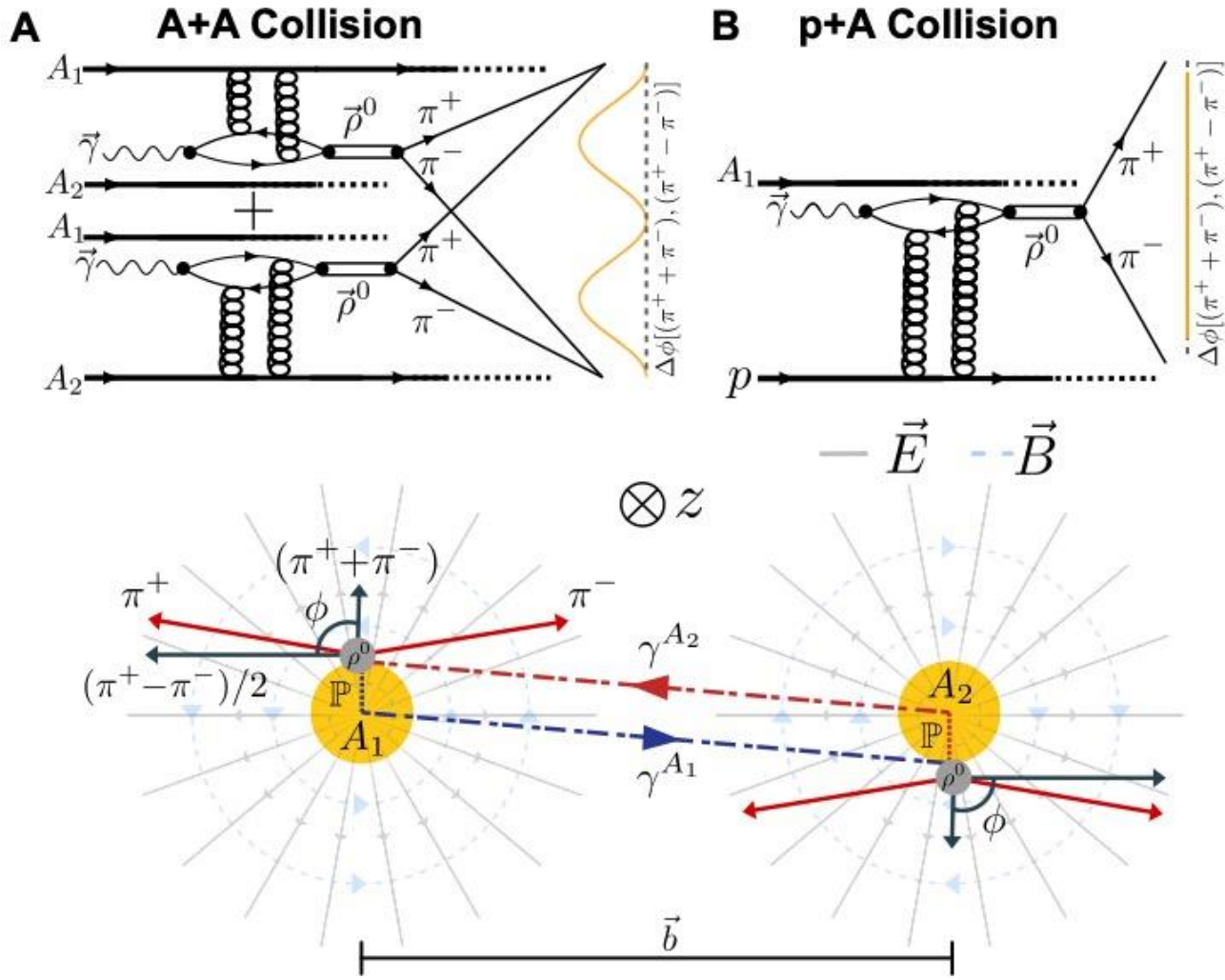

IF I have said that this is what reality is without any experimental evidence, most people would have thought that I am crazy.

"Truth is Stranger than Fiction,
but it is because Fiction is obligated
to stick to possibilities; Truth isn't."
– Mark Twain

Different type of entanglement and interference

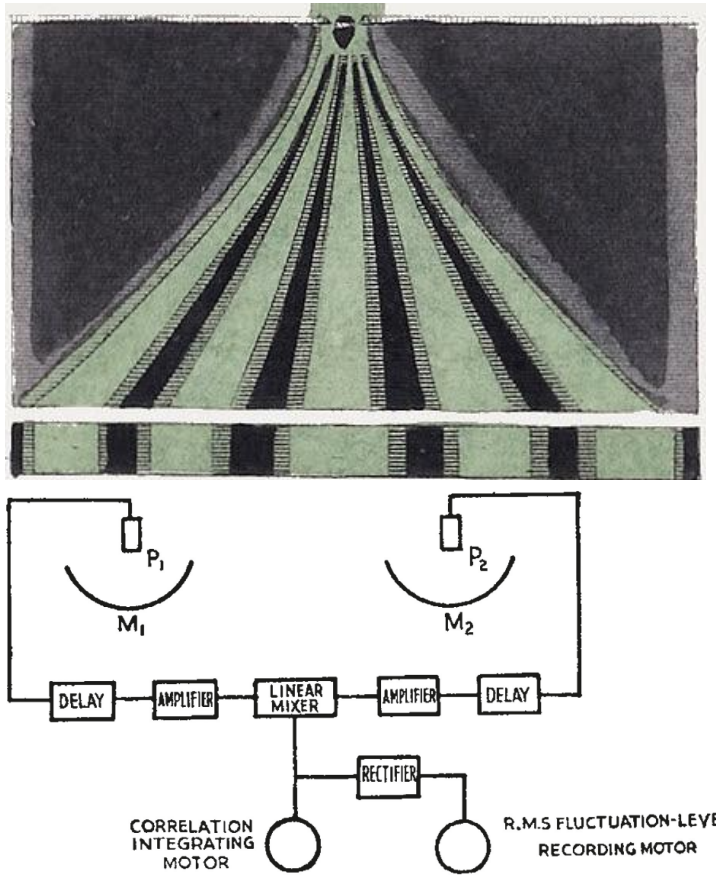

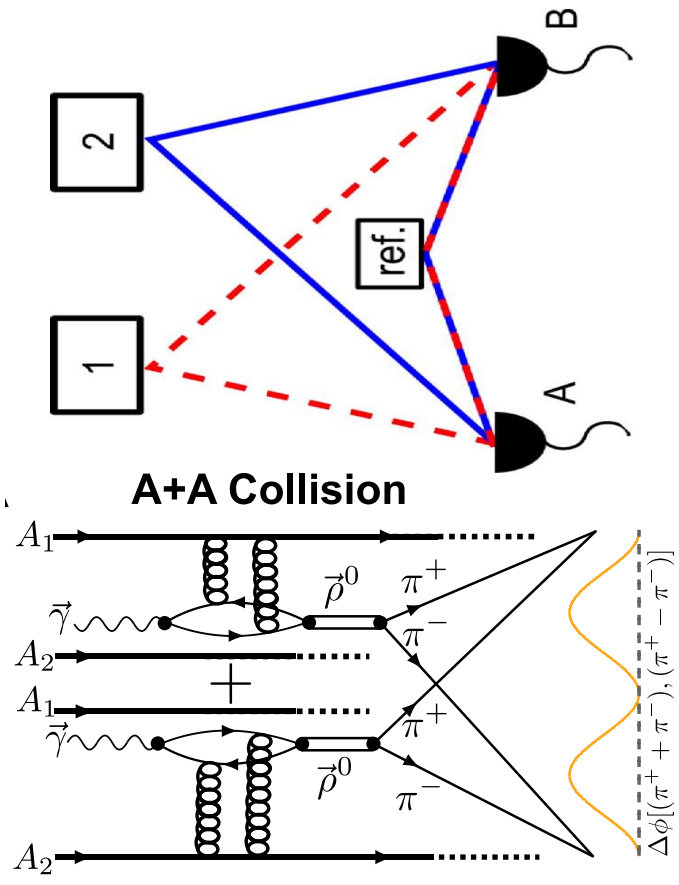

Top left: Observing interference pattern in the classical Young's double-slit experiment [71];

Bottom left: Detecting two photon coincidence in the HBT Intensity Interference [72, 73];

Top right: Detecting two photons with difference wavelengths from sources 1 and 2 at detectors A and B in the Entangled Enhanced Intensity Interference [48];

Bottom right: Detecting one pair of π^+ in the Entangled Enhanced Nuclear Tomography [69]. Plots are adapted from the references

Brandenburg, Klein, XZB, Yang, Zha, Zhou, Prog.Part.Nucl.Phys. 143 (2025) 104174

$\Delta\phi$ in Au+Au and U+U Collisions

A **STAR:** $\pi^+\pi^-$ Pairs, $P_T < 200$ MeV

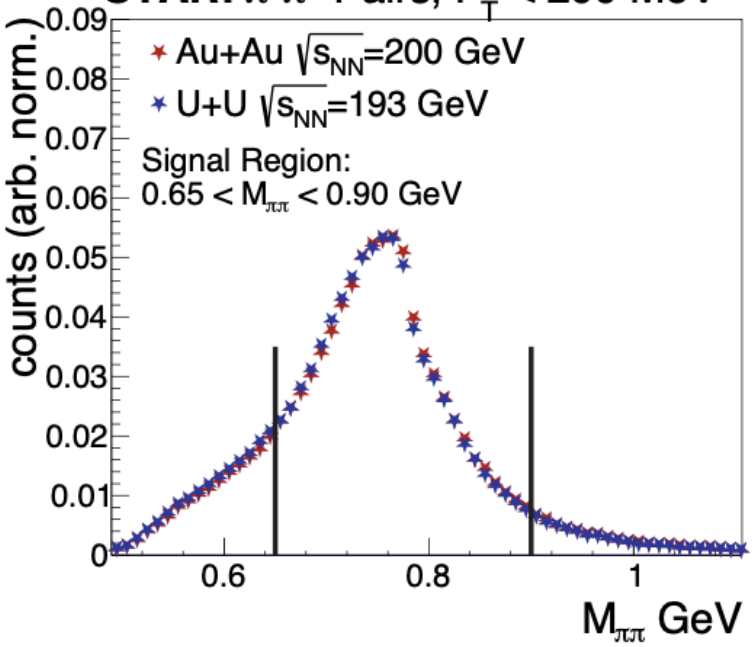

B **STAR:** Signal $\pi^+\pi^-$ pairs

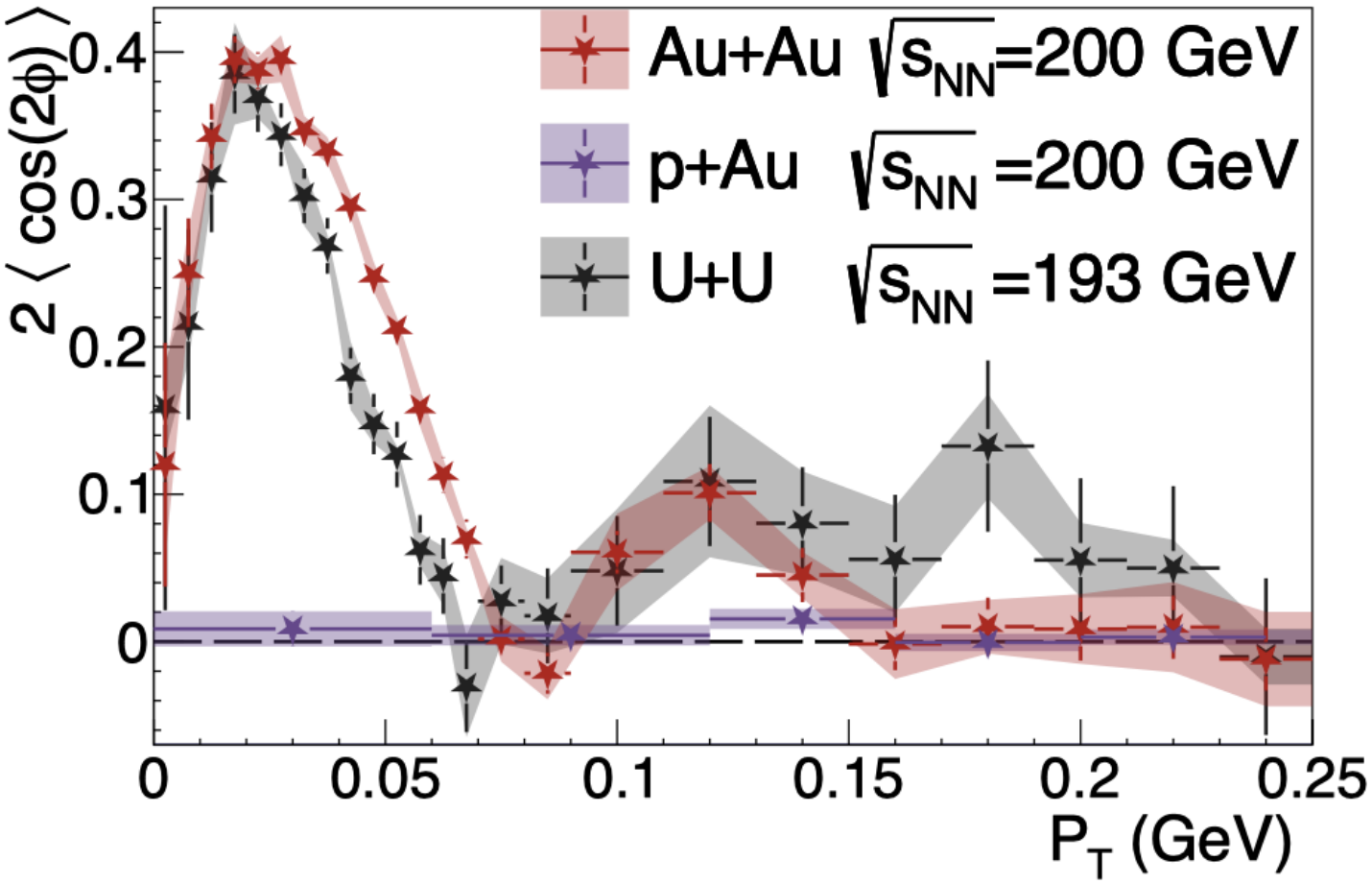

Quantify the difference in strength for Au+Au vs. U+U via a fit:

$$f(\Delta\phi) = 1 + a\ \cos 2\Delta\phi$$

Au+Au : $a = 0.292 \pm 0.004$ (stat) ± 0.004 (syst.)
U+U : $a = 0.237 \pm 0.006$ (stat) ± 0.004 (syst.)
Difference of 4.3σ (stat. & syst.):

arXiv:2204.01625

- Interference effect is sensitive to the nuclear geometry (gluon distribution) – difference between Au and U

Different radius from different angle?

Now instead of $+_{/}$ and $+_{1}$ lets look at $|5|$ with a 2D approach

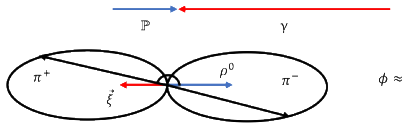

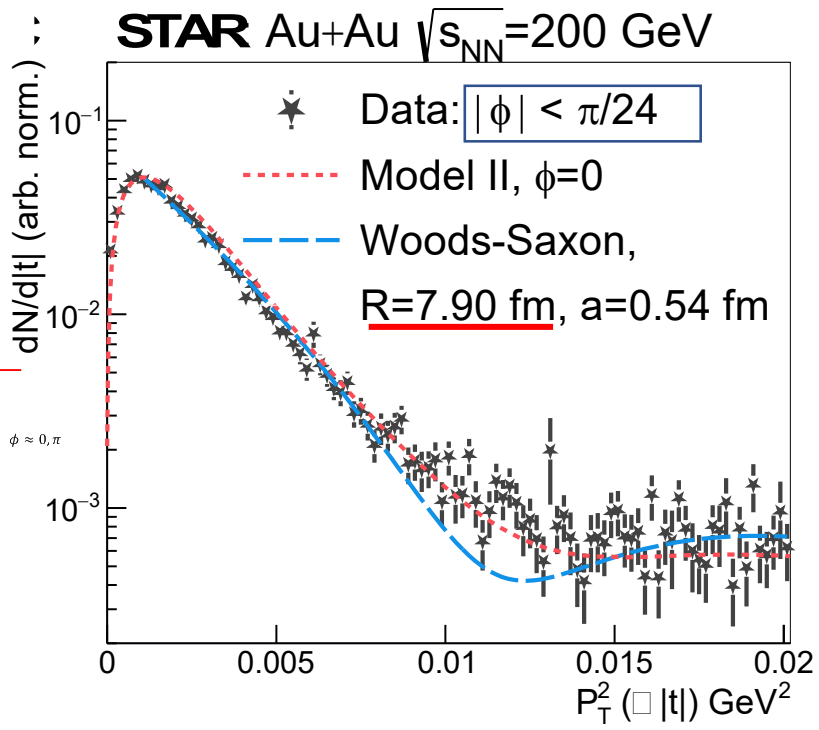

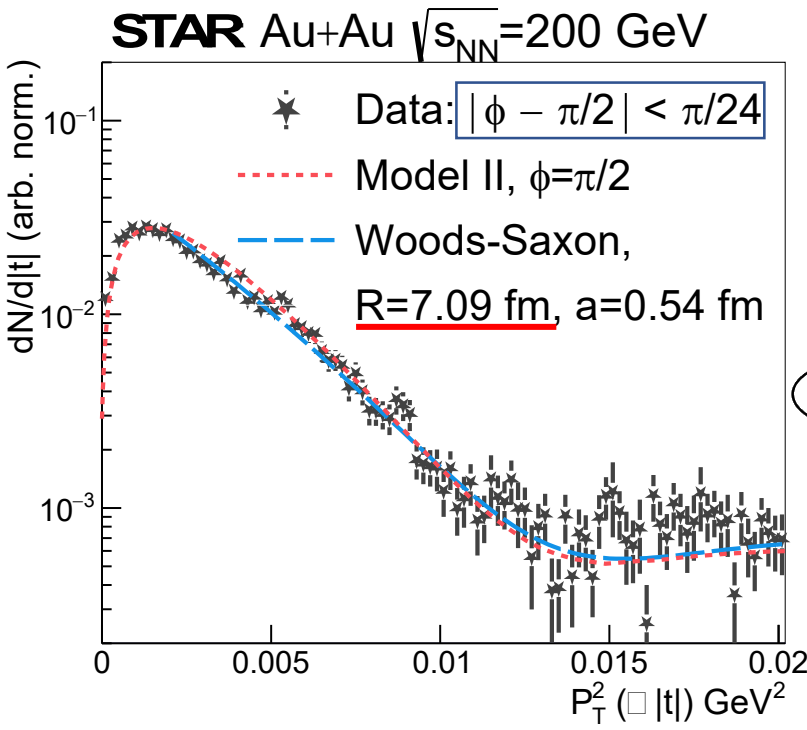

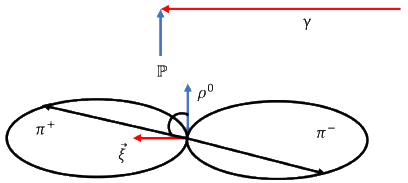

- Drastically different radius depending on ' , still way too big
- Notice how much better the Woods-Saxon dip is resolved for ' $= 6/2$ -> experimentally able to **remove photon momentum, which blurs diffraction pattern**
- **Can we extract the 'true' nuclear radius from |t| vs. 9 inforn**

arXiv:2204.01625

Precision radius measurement with interference

Azimuthal variation due to:

- Photon linear polarization,
- Spin transfer to VM
- Photon finite k_T
- VM spin 1 decay to spin 0 pions
- Interference along impact parameter

These image blurring effects can be improved with the angular dependence

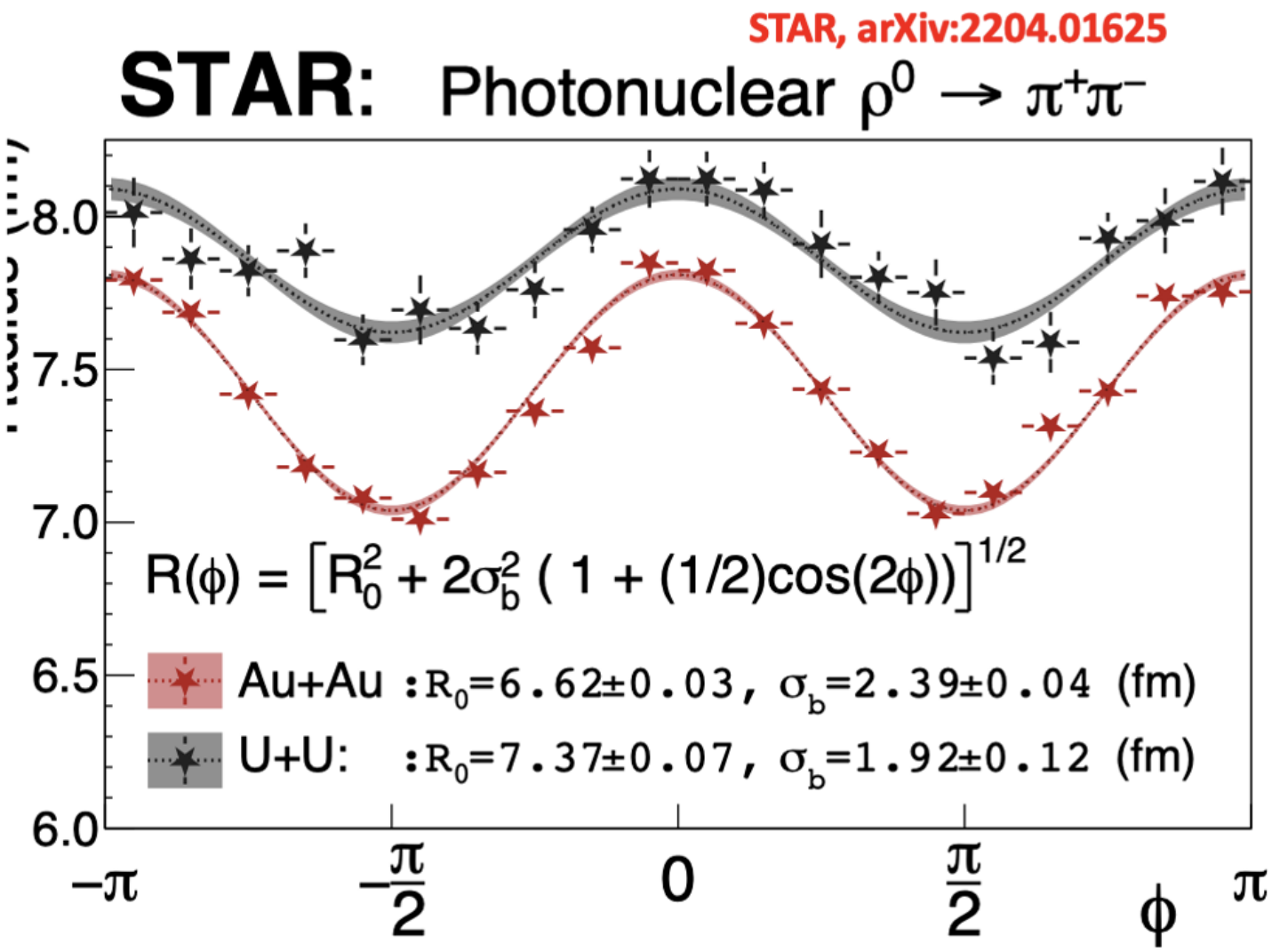

Extracted neutron skins and comparison to world data

	Au+Au (fm)	U+U (fm)
Charge Radius	6.38 (long: 6.58, short: 6.05)	6.81 (long: 8.01, short: 6.23)
Inclusive |t| slope (STAR 2017) [1]	7.95 ± 0.03	--
Inclusive |t| slope (WSFF fit)*	7.47 ± 0.03	7.98 ± 0.03
Tomographic technique*	6.53 ± 0.03 (stat.) ±0.05 (syst.)	7.29 ± 0.06 (stat.) ± 0.05 (syst.)
DESY [2]	6.45 ± 0.27	6.90 ± 0.14
Cornell [3]	6.74 ± 0.06	--
Neutron Skin (Tomographic Technique)*	0.17 ± 0.03(stat.) ±0.08(syst.) ~ 2σ	0.44 ± 0.05 (stat.) ±0.08 (syst.) ~ 4.7σ (Note: for Pb ≈ 0.3)

GIULIANO GIACALONE, July 22, 2022

$$\Delta r_{np} = 0.283 \pm 0.071 \text{ fm}$$

$$L = (106 \pm 37) \text{ MeV}$$

[PREX-II experiment, PRL **126** (2021) 17, 172502]

Stiffer EoS than expected.

[Reed et al., PRL **126** (2021) 17, 172503]
[Fattoyev et al., PRL **120** (2018) 17, 172702]

From GW170817

of $\Lambda_{1.4} \lesssim 580$ [44], we eagerly await the next generation of terrestrial experiments and astronomical observations to verify whether the tension remains. If so, the softening of the EOS at intermediate densities, together with the subsequent stiffening at high densities required to support massive neutron stars, may be indicative of a phase transition in the stellar core [42].

Can we get an independent estimate at RHIC?

M. Centelles, X. Roca-Maza, X. Viñas, and M. Warda
Phys. Rev. Lett. **102**, (2009) 122502

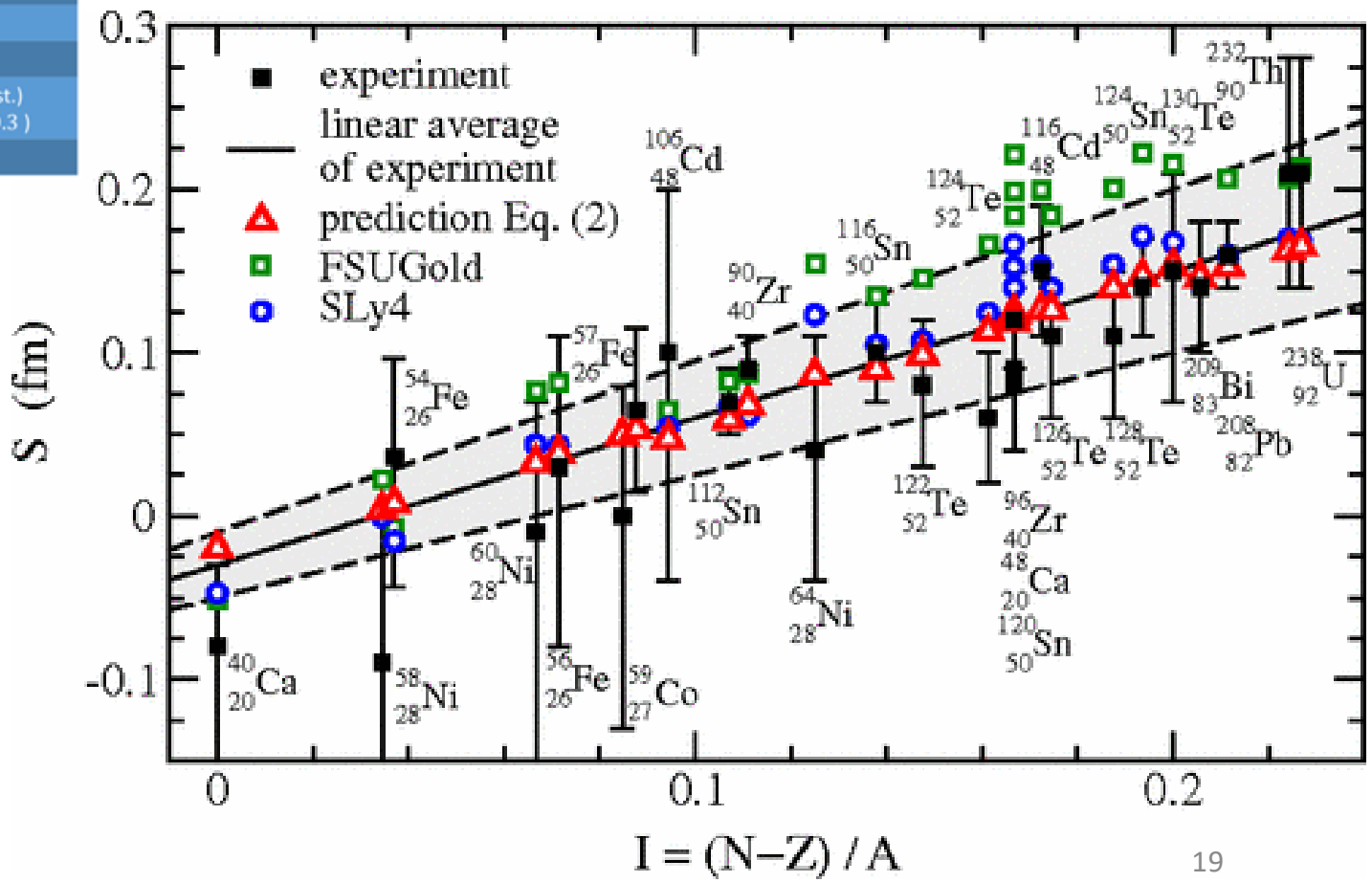

Extracted neutron skins and comparison to world data

	Au+Au (fm)	U+U (fm)
Charge Radius	6.38 (long: 6.58, short: 6.05)	6.81 (long: 8.01, short: 6.23)
Inclusive |t| slope (STAR 2017) [1]	7.95 ± 0.03	--
Inclusive |t| slope (WSFF fit)*	7.47 ± 0.03	7.98 ± 0.03
Tomographic technique*	6.53 ± 0.03 (stat.) ±0.05 (syst.)	7.29 ± 0.06 (stat.) ± 0.05 (syst.)
DESY [2]	6.45 ± 0.27	6.90 ± 0.14
Cornell [3]	6.74 ± 0.06	--
Neutron Skin (Tomographic Technique)*	0.17 ± 0.03(stat.) ±0.08(syst.) ~ 2σ	0.44 ± 0.05 (stat.) ±0.08 (syst.) ~ 4.7σ (Note: for Pb ≈ 0.3)

GIULIANO GIACALONE, July 22, 2022

$$\Delta r_{np} = 0.283 \pm 0.071 \text{ fm}$$

$$L = (106 \pm 37) \text{ MeV}$$

[PREX-II experiment, PRL **126** (2021) 17, 172502]

Stiffer EoS than expected.

[Reed et al., PRL **126** (2021) 17, 172503]
[Fattoyev et al., PRL **120** (2018) 17, 172702]

From GW170817

of $\Lambda_{1.4} \lesssim 580$ [44], we eagerly await the next generation of terrestrial experiments and astronomical observations to verify whether the tension remains. If so, the softening of the EOS at intermediate densities, together with the subsequent stiffening at high densities required to support massive neutron stars, may be indicative of a phase transition in the stellar core [42].

Can we get an independent estimate at RHIC?

M. Centelles, X. Roca-Maza, X. Viñas, and M. Warda
Phys. Rev. Lett. **102**, (2009) 122502

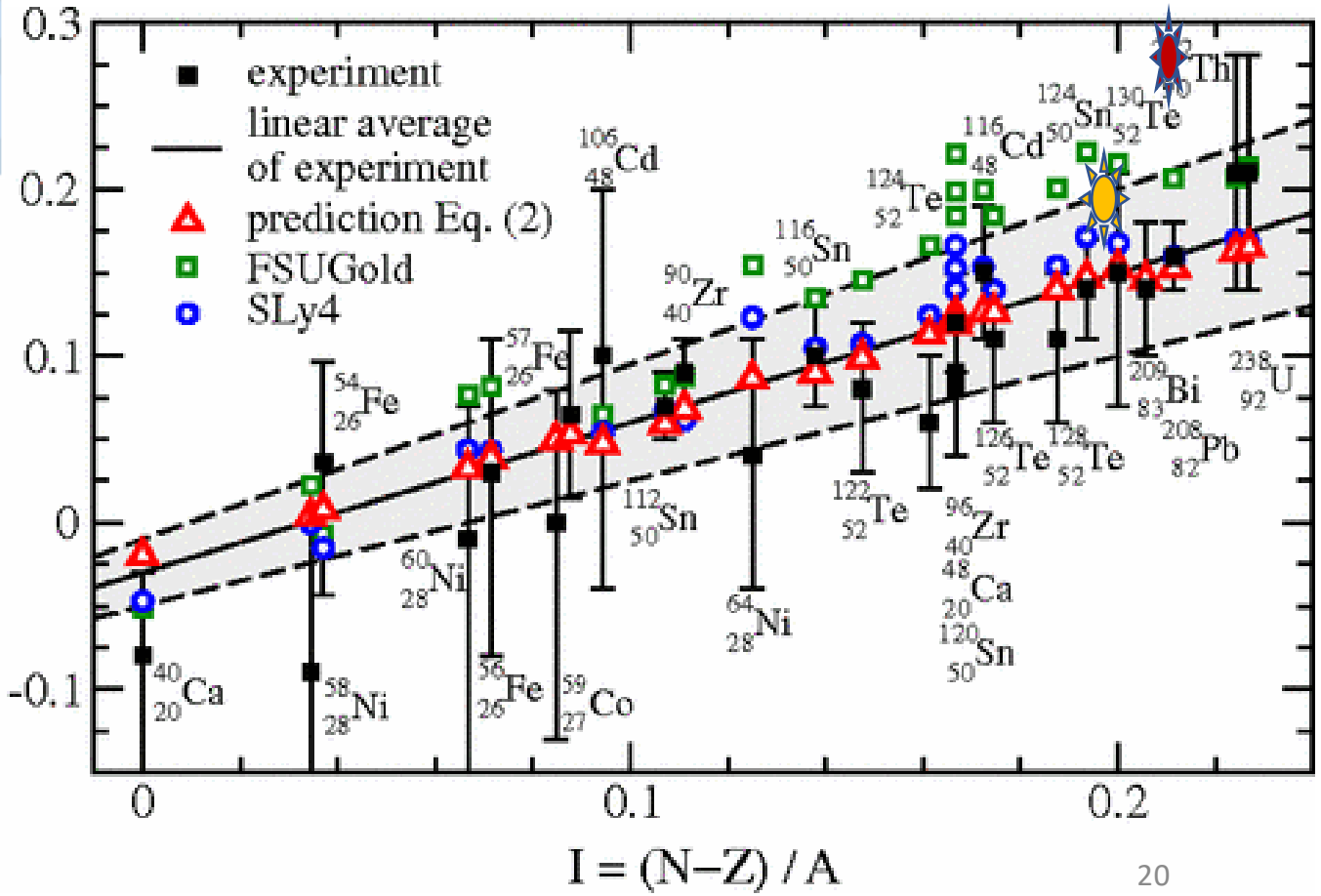

Comparison to models

Comparison to models with the interference effect

- Model I:
  VM production cross section from HERA ep data
  Glauber with smooth NN overlap function
- Model II:
  dipole model with gluon saturation in A+A

STAR, arXiv:2204.01625

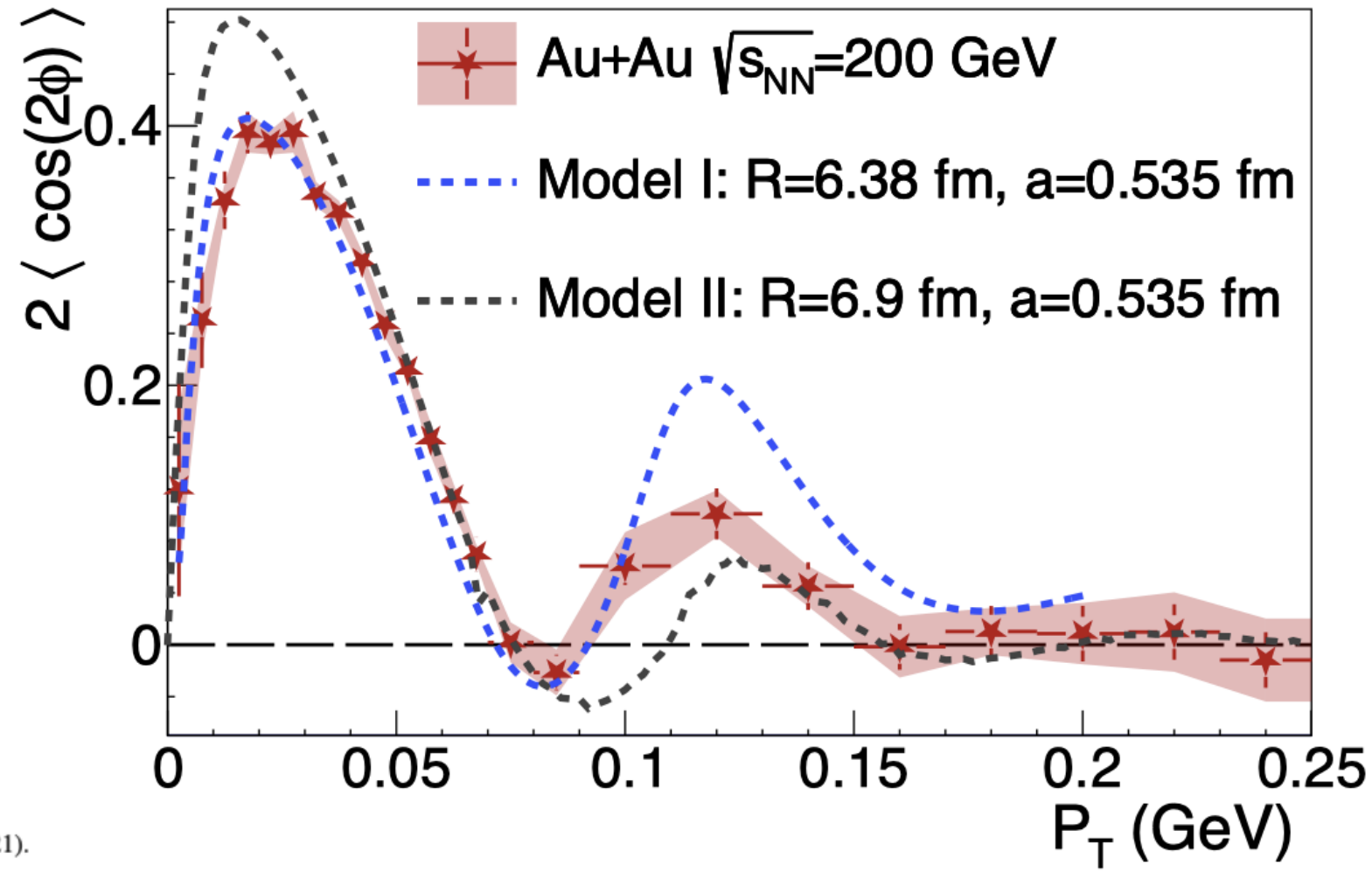

W. Zha, L. Ruan, Z. Tang, Z. Xu, S. Yang, *Phys. Rev. C* **99**, 061901 (2019).

W. Zha, J. D. Brandenburg, L. Ruan, Z. Tang, *Phys. Rev. D* **103**, 033007 (2021).

H. Xing, C. Zhang, J. Zhou, Y.-J. Zhou, *JHEP* **10**, 064 (2020).

Extracting deformation in ^{238}U

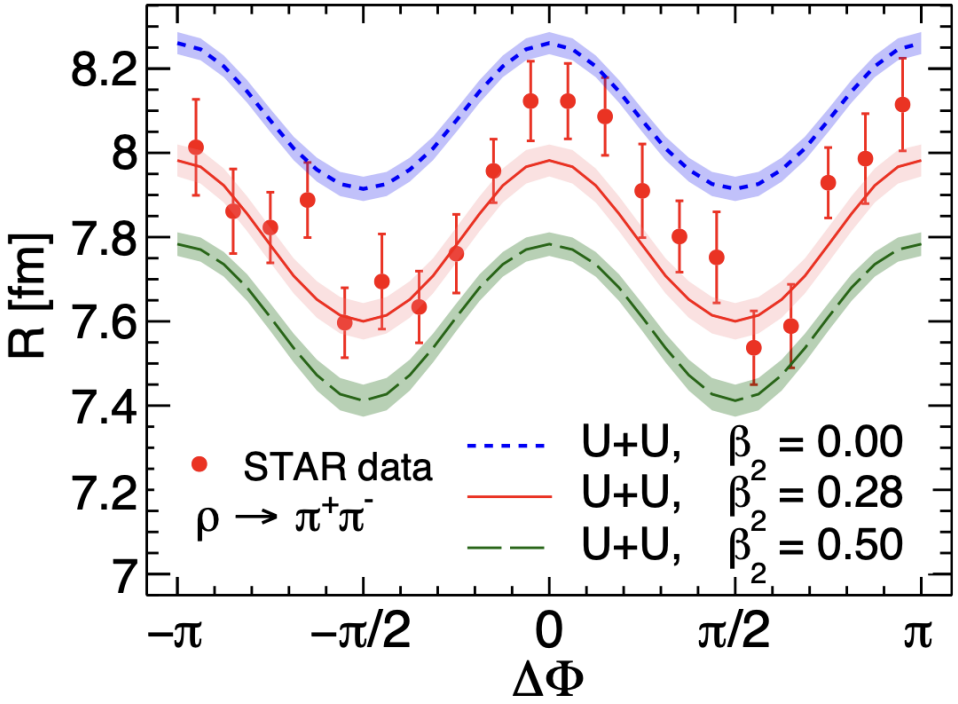

FIG. 8. The effective radius obtained from a fit using Eq. (16) as a function of the $\Phi_P - \Phi_q$ angle for U+U with different β_2 values. The bands indicate the uncertainties from extracting the radius. The STAR data is from [29].

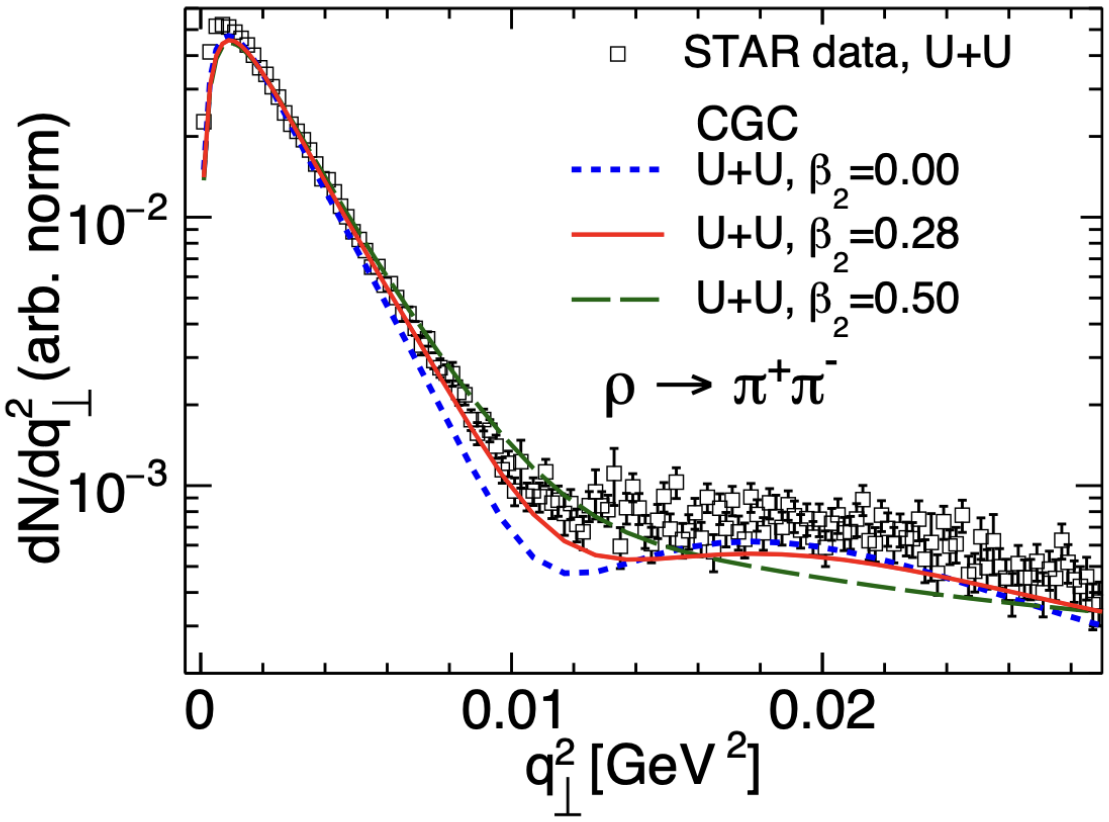

FIG. 4. The $\mathrm{d}N/\mathrm{d}q_\perp^2$ as a function of $q_\perp^2$ for U+U collisions with different β_2 values averaged over $\Delta\Phi$. The STAR data is from [29].

Effects of nuclear structure and quantum interference on diffractive vector meson production in ultra-peripheral nuclear collisions
Heikki Mäntysaari, Farid Salazar, Björn Schenke, Chun Shen, Wenbin Zhao
Phys.Rev.C 109 (2024) 2, 024908; e-Print: 2310.15300 [nucl-th]

Improvements of future measurements

- Both interference and Woods-Saxon models only describe the first peak well

- The neutron skin syst. uncertainty mainly due to WS vs Gaussian,
  and the actual distribution seems to be flatter (more prominent second peak)

W. Zha, L. Ruan, Z. Tang, Z. Xu, S. Yang, *Phys. Rev. C* **99**, 061901 (2019).

W. Zha, J. D. Brandenburg, L. Ruan, Z. Tang, *Phys. Rev. D* **103**, 033007 (2021).

H. Xing, C. Zhang, J. Zhou, Y.-J. Zhou, *JHEP* **10**, 064 (2020).

Coherent diffractive VM preserves spin alignment of photon
Incoherent does NOT

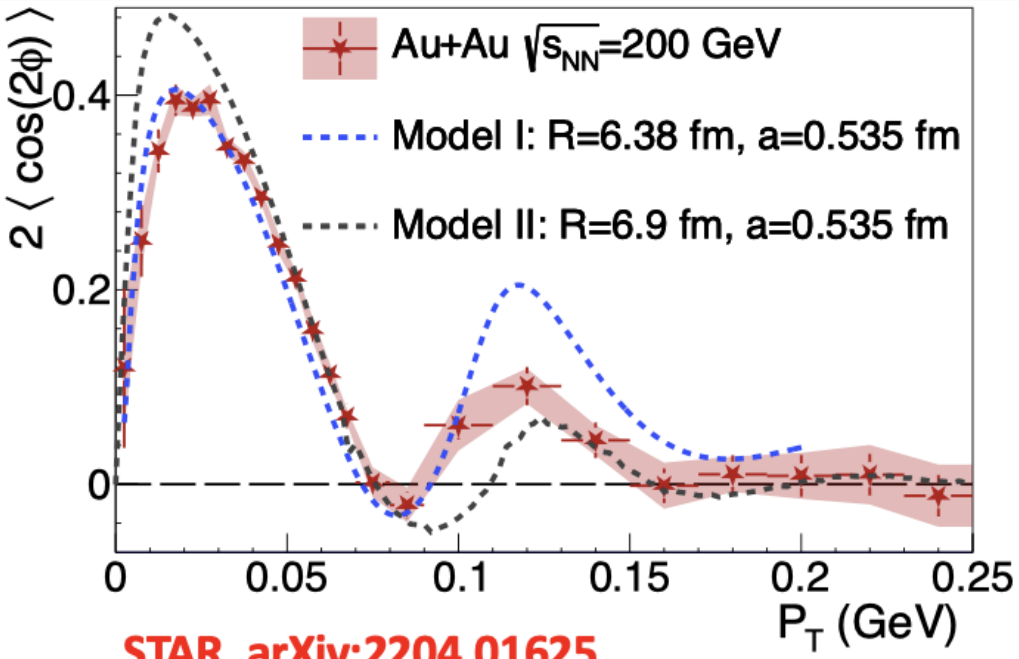

STAR, arXiv:2204.01625

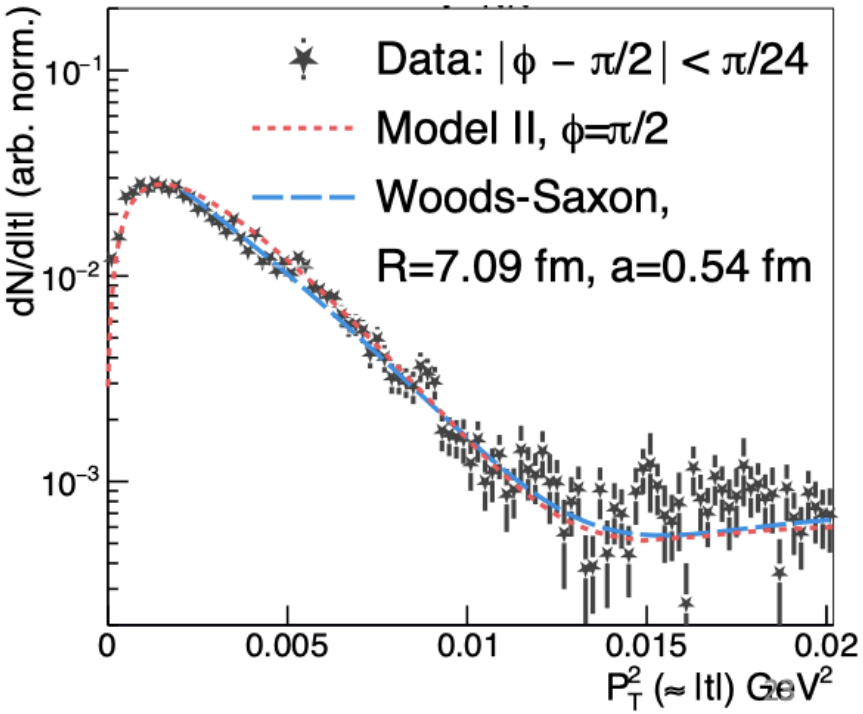

Heavier vector meson (J/ψ)

Accepted by PRL

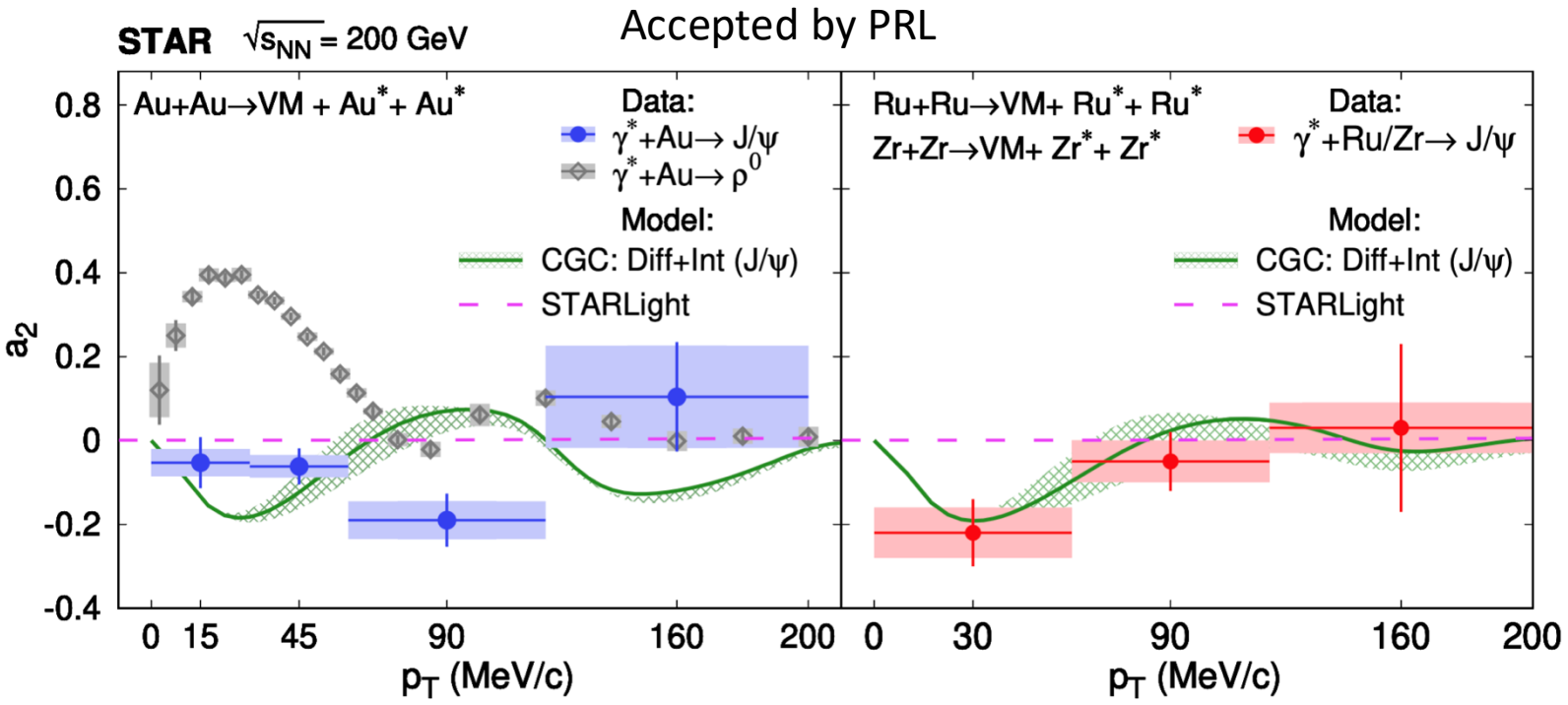

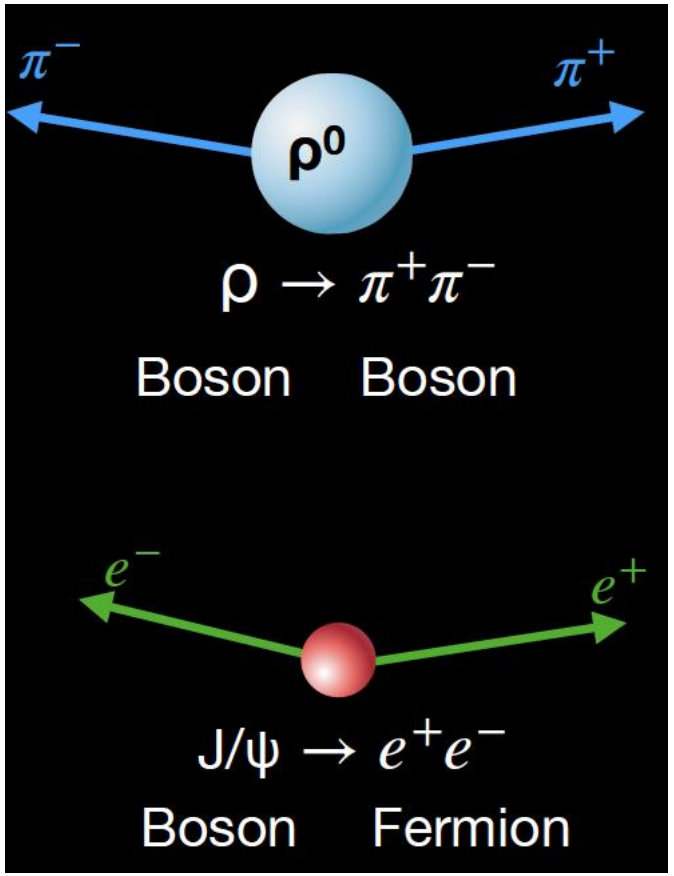

Diff+Int predictions : Mäntysaari et al. Phys.Rev.C 109 (2024) 2, 024908
Ashik Sheikh, APS GHP, March 2025

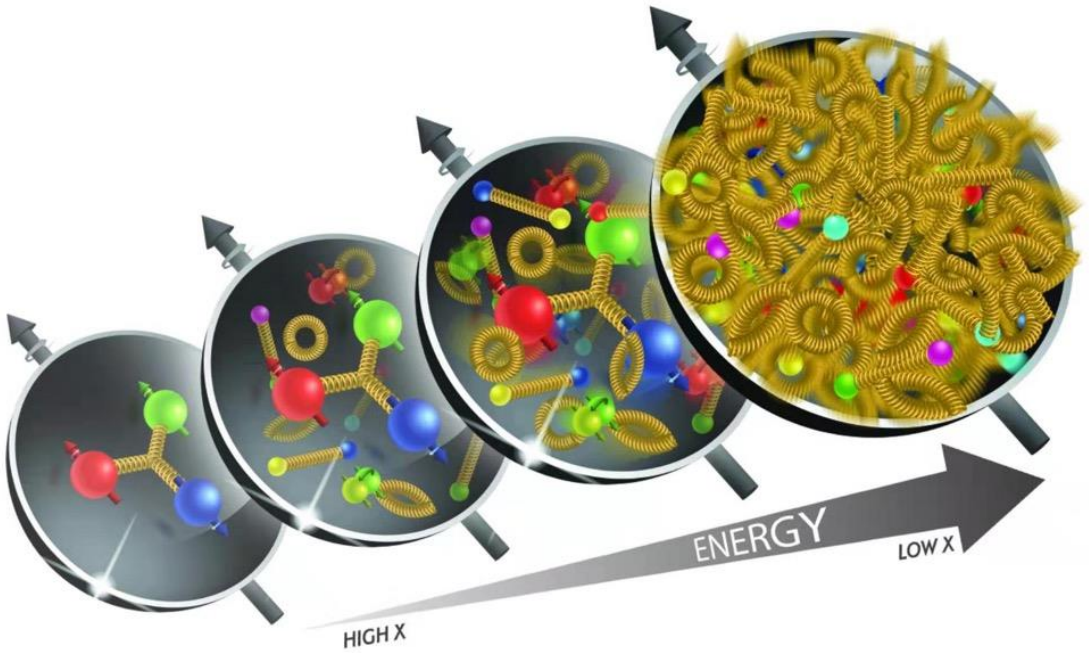

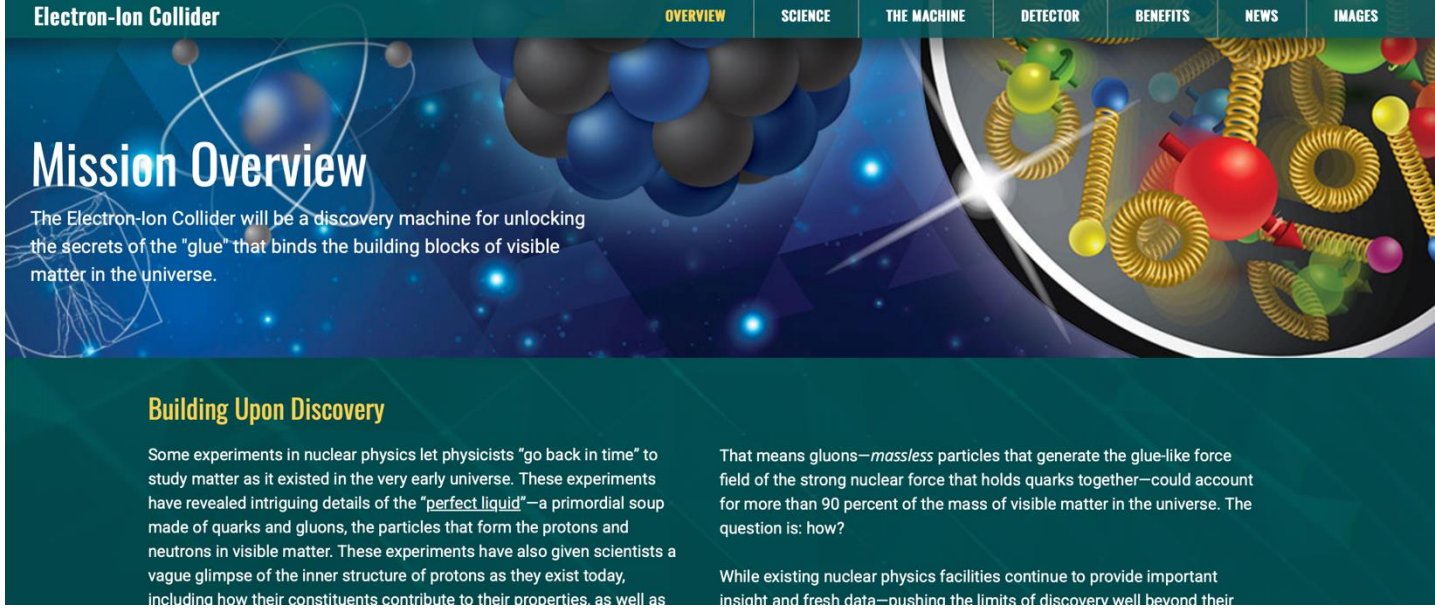

Next Big thing in USA – The Electron-Ion Collider (EIC)

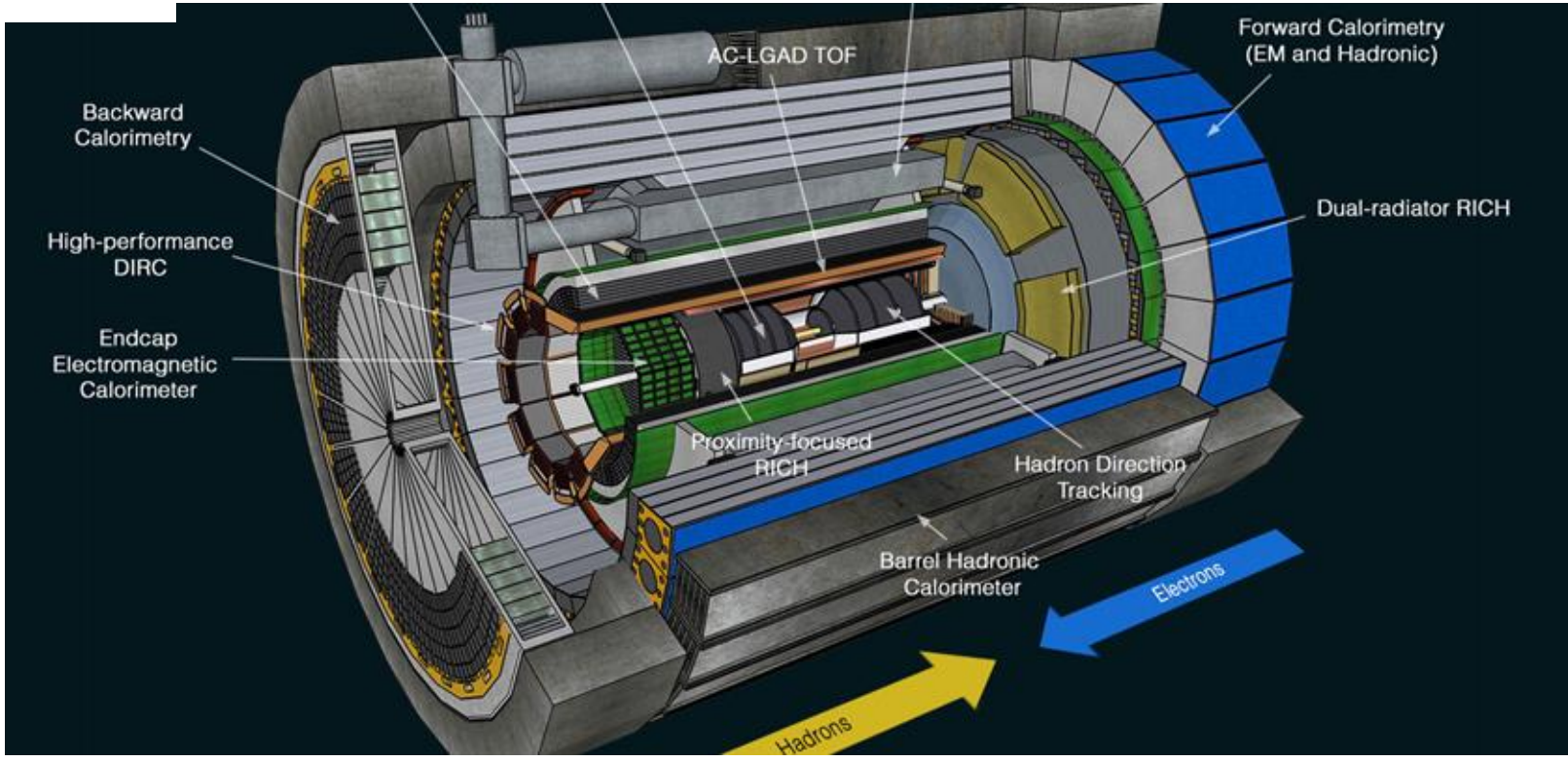

ePIC

Published April 6, 2026 | Version v4

Report Open

Analysis Note: Precision Extraction of Momentum Transfer in Diffractive Coherent Exclusive Vector Meson Production

Maci Kesler (Contact person)[1]; Ashik Ikbal Sheikh[1]; Rongrong Ma[2]; Zhoudunming Tu[2]; Thomas Ullrich[2]; Zhangbu Xu[2, 1]

Show affiliations

Analysis note for the study of extracting the momentum transfer distribution measurement through coherent exclusive diffractive vector meson production.

Files

epic-AN-AC-2025-001.v2.pdf

38 of 39 — Automatic Zoom

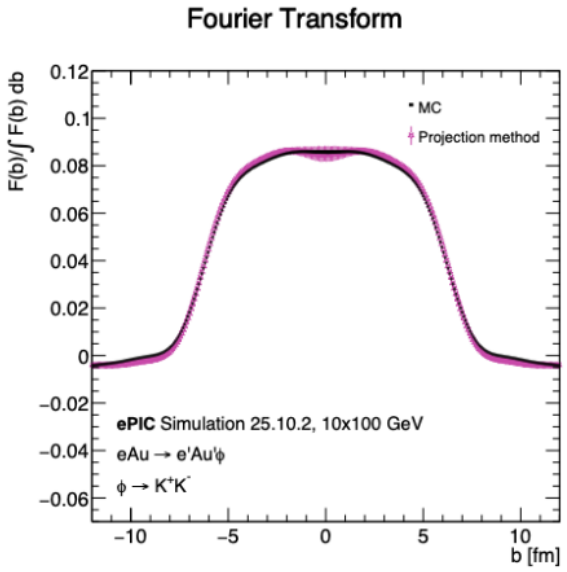

Figure 36: Gluon spatial distribution from the Fourier transformation of the MC $|t|$ distribution, shown as the black curve and from the projection method with a wedge cut of $\omega_{max} = \pi/12$ shown as the open pink stars.

Nuclear size grows with saturation

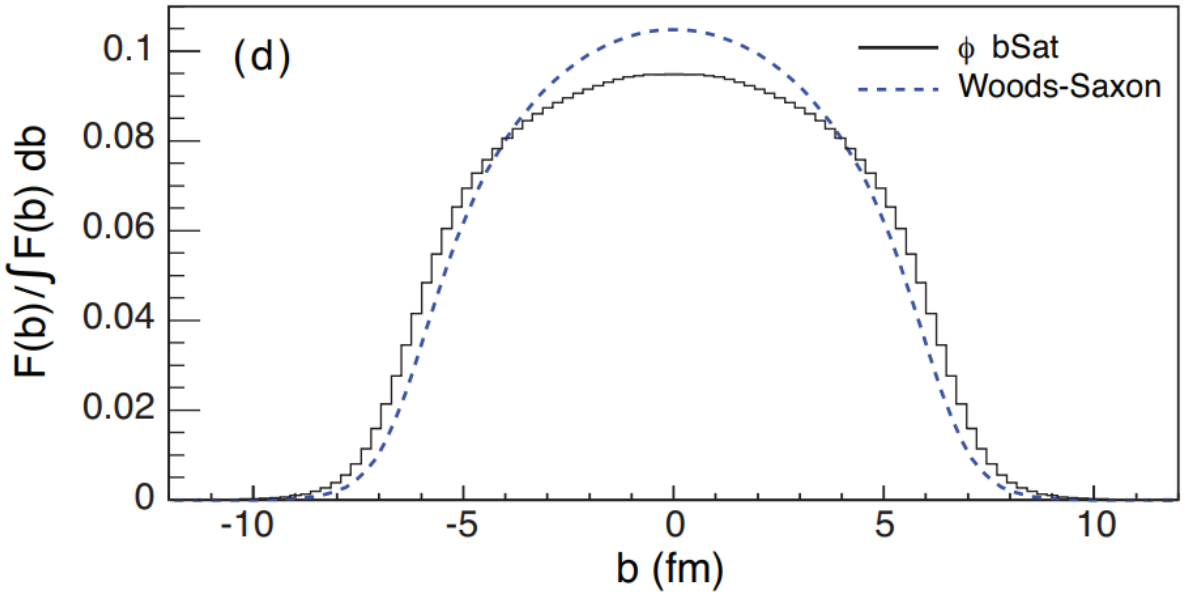

Projective Nuclear Tomography through exclusive vector meson production in e+A

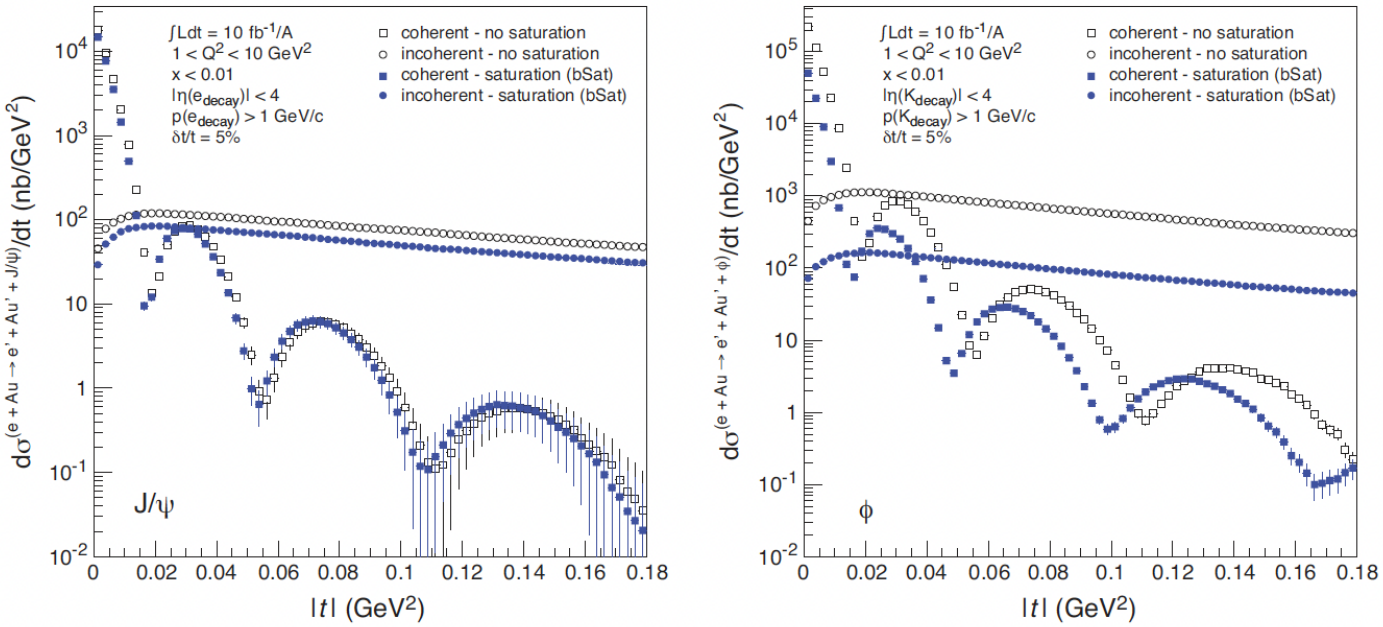

Figure 3.23: $d\sigma/dt$ distributions for exclusive J/ψ (left) and ϕ (right) production in coherent and incoherent events in diffractive e+Au collisions. Predictions from saturation and non-saturation models are shown.

- Exclusive coherent vector meson production on |t| distribution sensitive to the geometry (gluon) distribution at high energy (low-x)
- One of the must-do measurements at EIC
- However, two issues:
  |t| resolution is too bad
  incoherent background too high

Electron Ion Collider: The Next QCD Frontier : Understanding the glue that binds us all, *Eur.Phys.J.A* 52 (2016) 9, 268

Science Requirements and Detector Concepts for the Electron-Ion Collider : EIC Yellow Report, *Nucl.Phys.A* 1026 (2022) 122447

Projective Nuclear Tomography through exclusive vector meson production in e+A

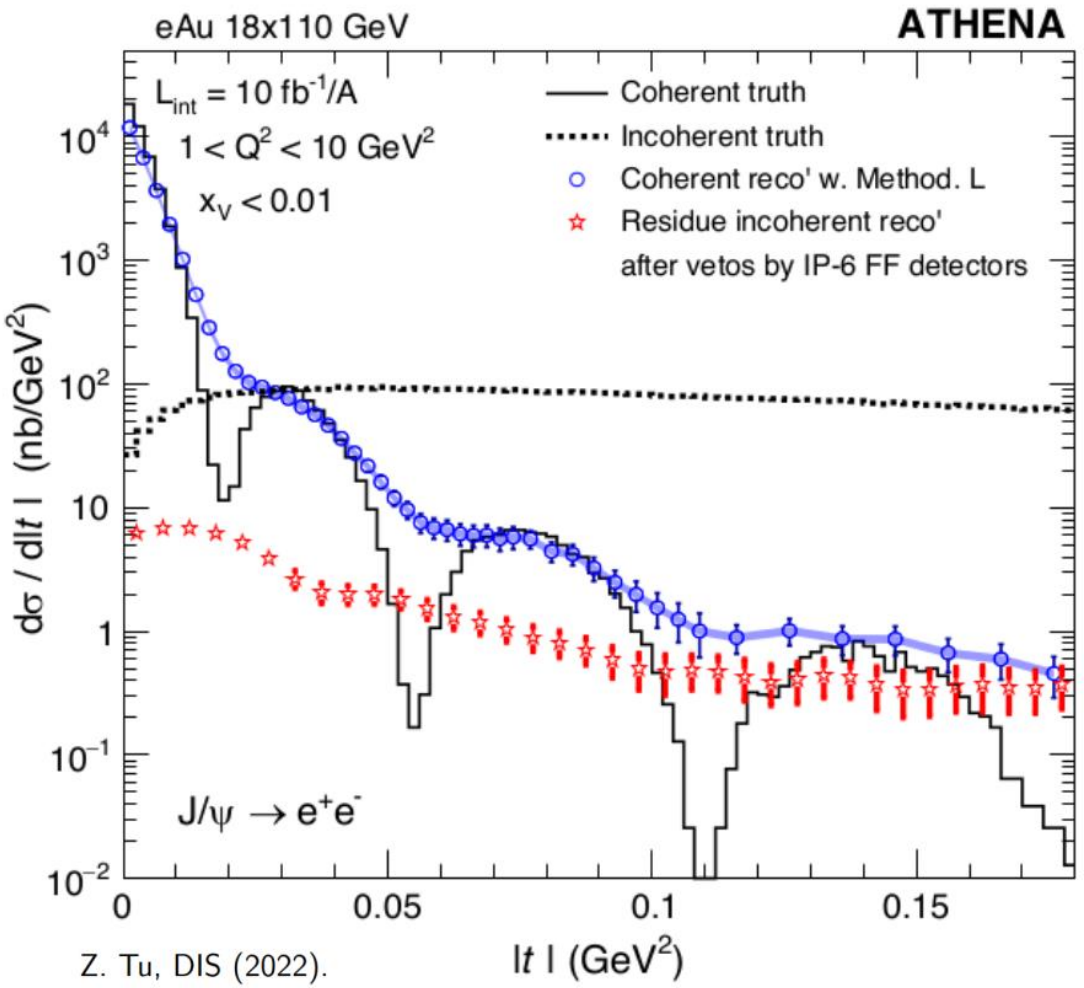

- Exclusive coherent vector meson production on |t| distribution sensitive to the geometry (gluon) distribution at high energy (low-x)
- One of the must-do measurements at EIC
- However, two issues:
  |t| resolution is too bad
  incoherent background too high

Extracting t: $e + A \rightarrow e' + A' + V$

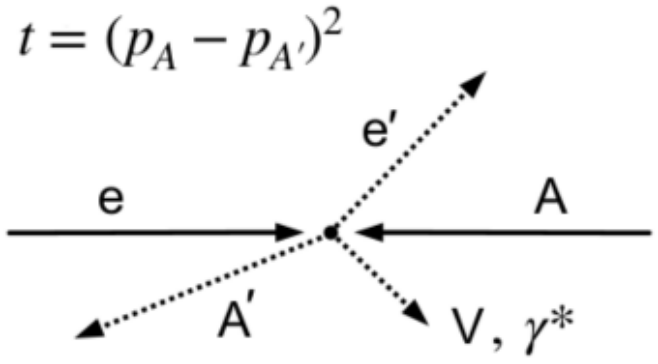

- To access t: need complete final state
  - Cannot measure $p_{A'}$
- Know 4-momenta of e, A, e', and V
- Different methods to do this

T. Ullrich, (2020).

- Method E: gives true $t = (p_V + p_{e'} - p_e)^2$
  - Cons: Subtract large incoming/outgoing momenta to get longitudinal component of t → small error/inaccuracy has large effect on t
- Method A: ignores longitudinal momenta $t = [p_T(e') + p_T(V)]^2$
  - Cons: underestimates true t, valid only for small t and small Q^2
- Method L: improvement to Method E, corrects $p_{A'}$ and uses true invariant mass to compensate the smearing $t_{corr} = |p_A - p_{A'}^{corr}|^2$
  - Cons: only applies to coherent events

New Method

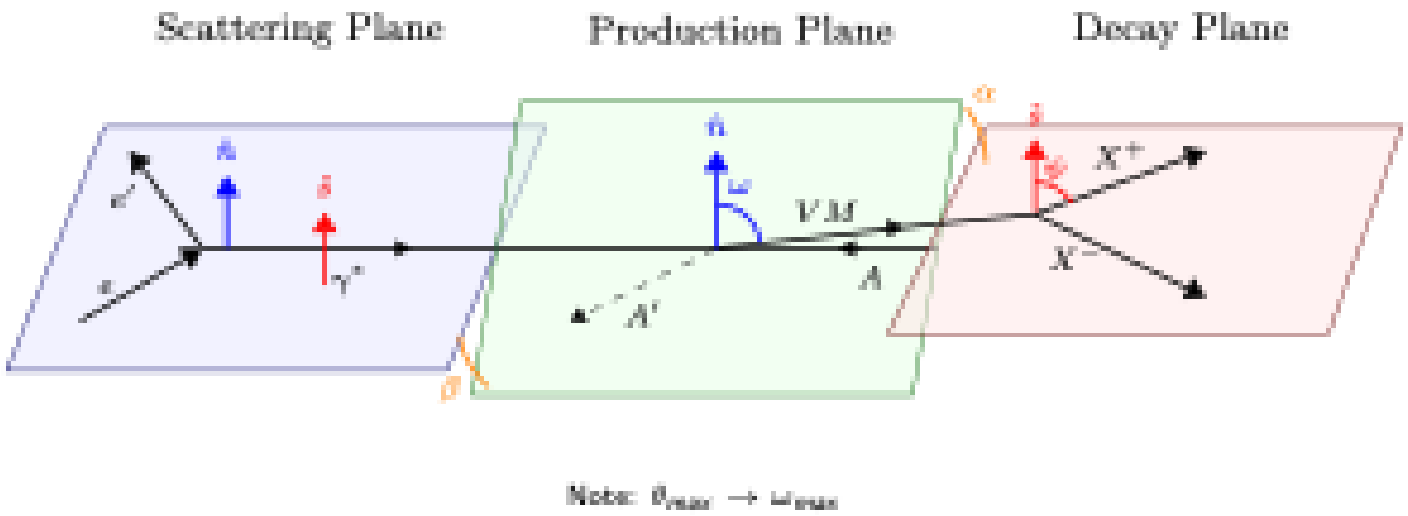

Note: $\theta_{recoil} \rightarrow \omega_{recoil}$

- Measure $|t|$ component along normal direction ($\hat{n}$) of electron scattering plane
- $|t|_{\hat{n}}$ unaffected by momentum resolution
  - Eliminate momentum resolution contribution from e'

Define $\hat{n}$:

$$\hat{n} = \hat{p}_e \times \hat{p}_{e'}$$

arXiv:2502.15596

College of Arts & Sciences

Future Students | Undergraduate | Graduate | Departments & Schools | Degree Programs | Research | Support the College

DOE Award Winner Paving the Way for Future Breakthroughs

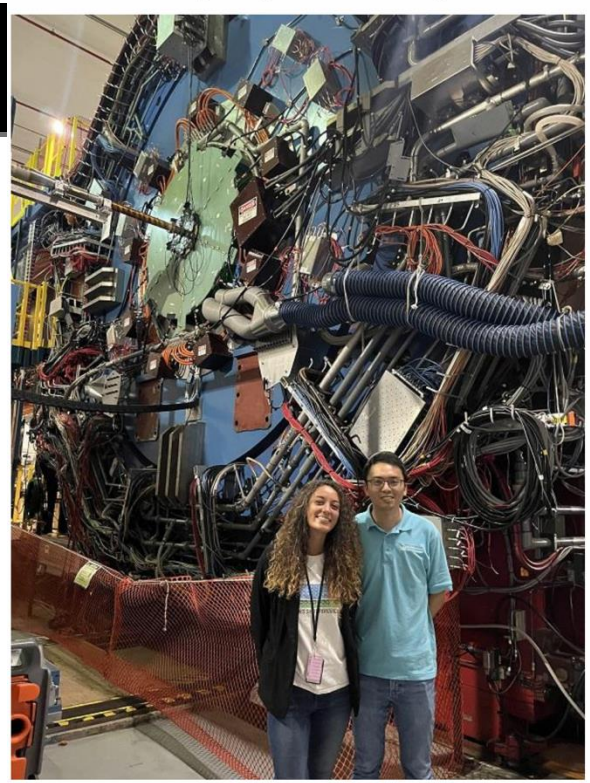

Maci Kesler (left) with her mentor at Brookhaven (Rongrong Ma)

Although Maci Kesler grew up in Tiffin, Ohio, her collegiate academic path began in Las Vegas, where she earned her bachelor's degree from UNLV. Today, her influence reaches all the way to Brookhaven. Now a third-year Ph.D. student, she is leading a highly specialized detector simulation project for a new particle accelerator scheduled to launch in the 2030s. The project is part of the U.S. Department of Energy's ambitious plan to build the Electron-Ion Collider at Brookhaven National Laboratory — a next-generation facility designed to help scientists explore the inner structure of protons and neutrons.

Kesler's research focuses on improving a complex measurement method that had been mostly abandoned due to experimental detection challenges. Working closely with Brookhaven scientists, she found a new way to revive one of the "must-do" projects in imaging the inner structure of heavy nuclei to understand how the strong-force carrier (gluon) behaves inside a large nucleus. Because of her expertise and leadership, she is now the main contact for this part of the ePIC Collaboration, an international collaboration of over 1,000 scientists.

She is also a recipient of the prestigious SCGSR Award from the Department of Energy, which supports her research and gives her opportunities to travel, collaborate and present her work.

Match our simulation to the EIC detector resolution

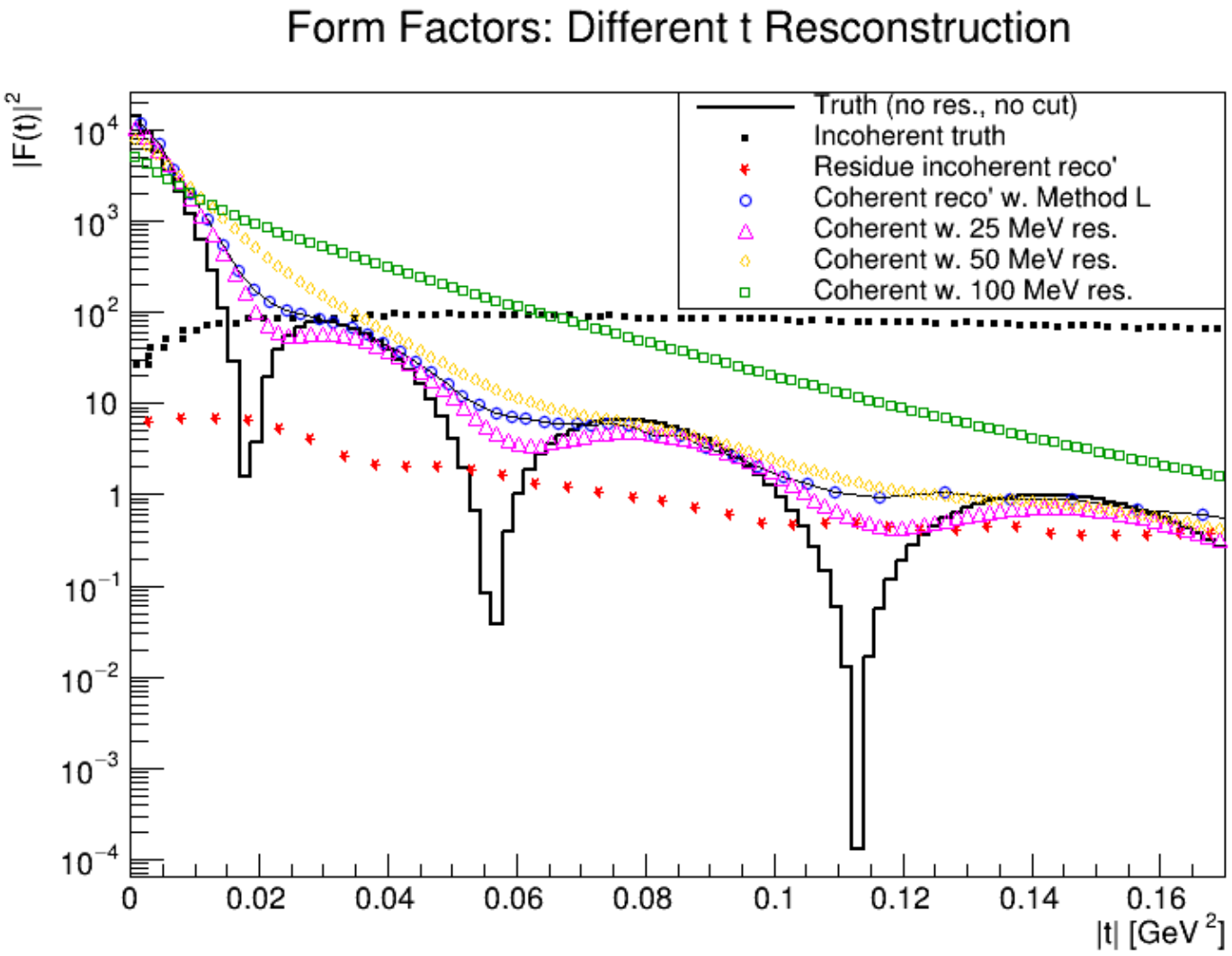

- Tune the |t| resolution to match the EIC detector simulation resolution:

  $(25—50\text{MeV})^2$

Maci Kesler, *et al.,* e-Print: 2502.15596

In 2D

$$f(t_x + ty) = f(t_y) + \frac{df(ty)}{dt_x}dt_x + \frac{d^2f(ty)}{d^2t_x}(dt_x)^2$$

$$\frac{df(ty)}{dt_x}=0; \quad = f(t_y)\,|_{tx=0} + \frac{d^2f(ty)}{d^2t_x}(dt_x)^2 = f(t_y) + f(t_y)(dt_x/t_y)^2$$

Form factor is isotropic in 2D since pomeron is spin 0

Detector resolution smears the x component

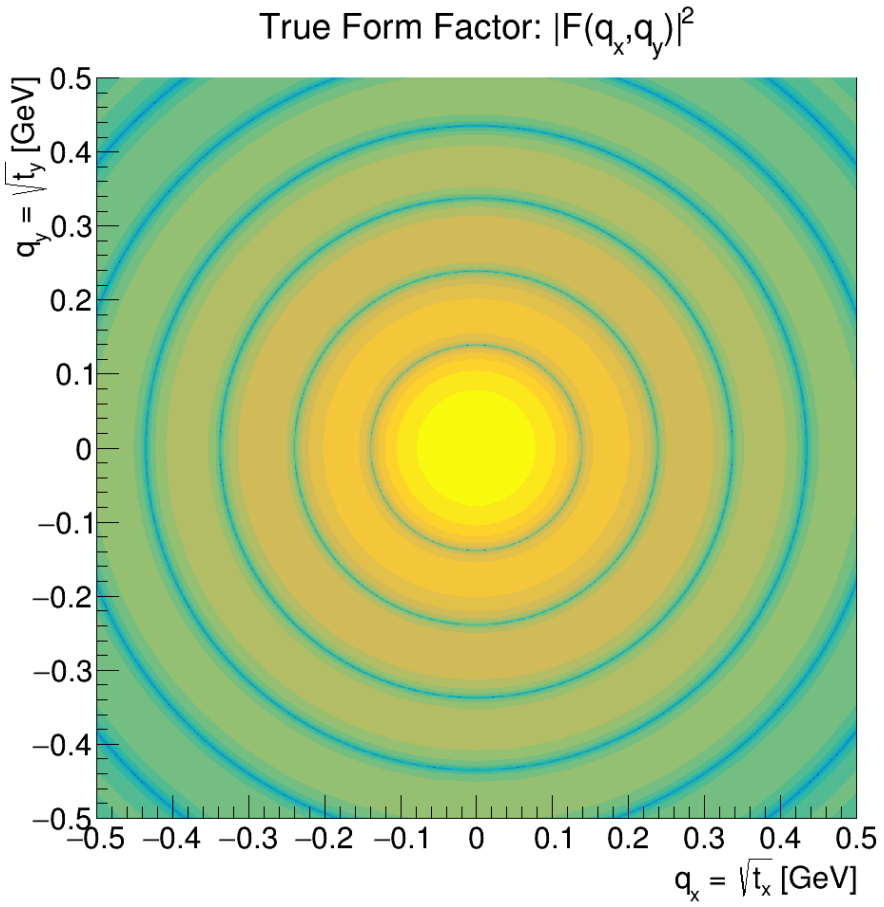

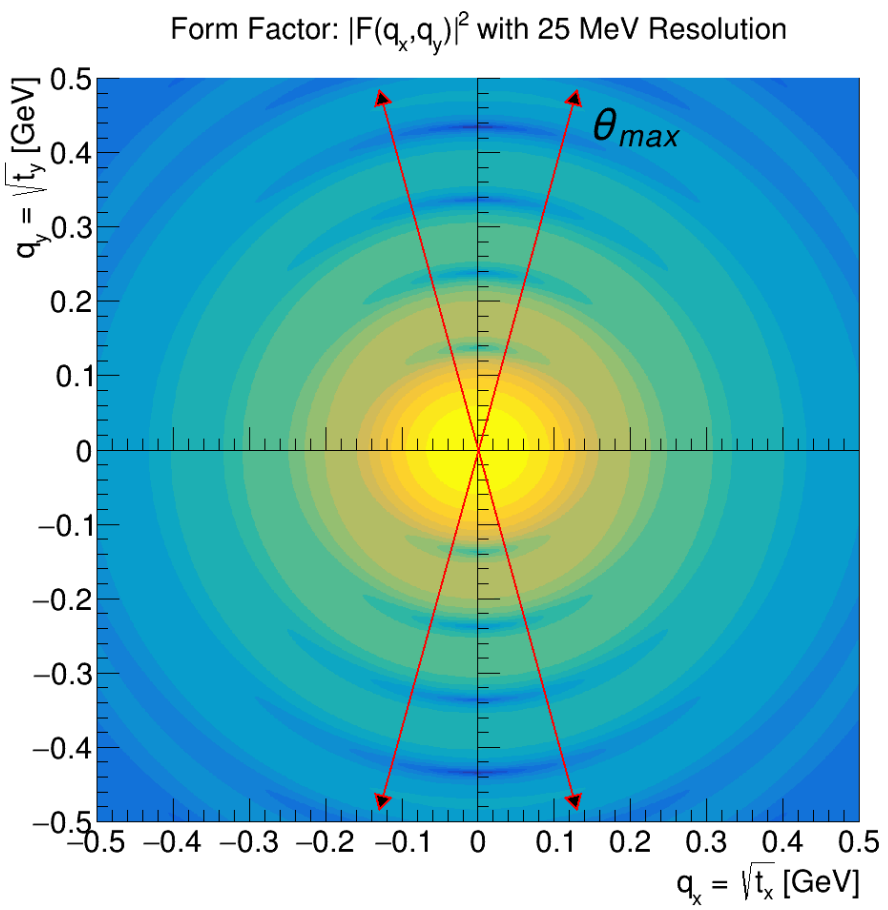

Maci Kesler, *et al.,* e-Print: 2502.15596

Selection on specific projection

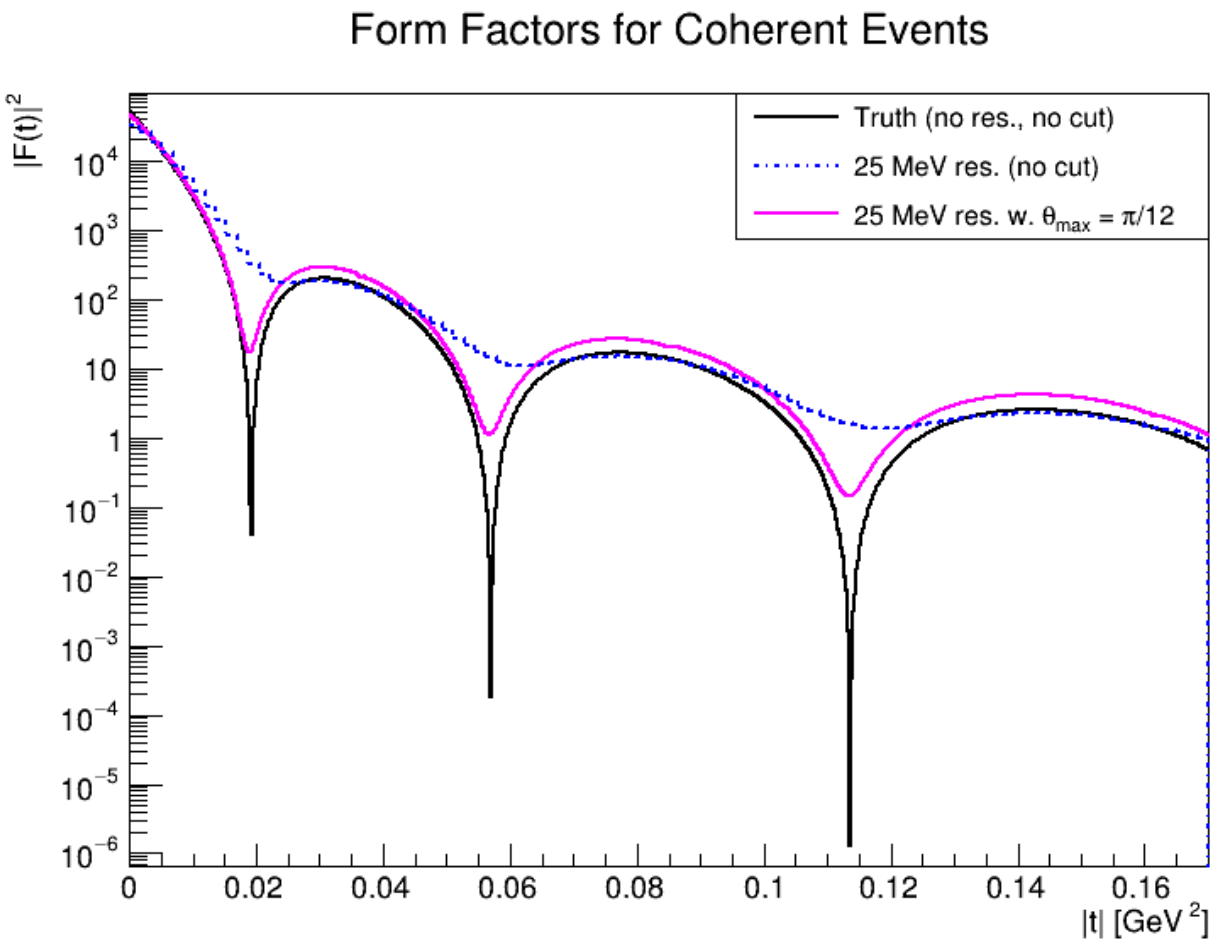

- Selection of a wedge along the y component avoids the detector resolution

Maci Kesler, *et al.,* e-Print: [2502.15596]

Projective Nuclear Tomography through exclusive vector meson production in e+A

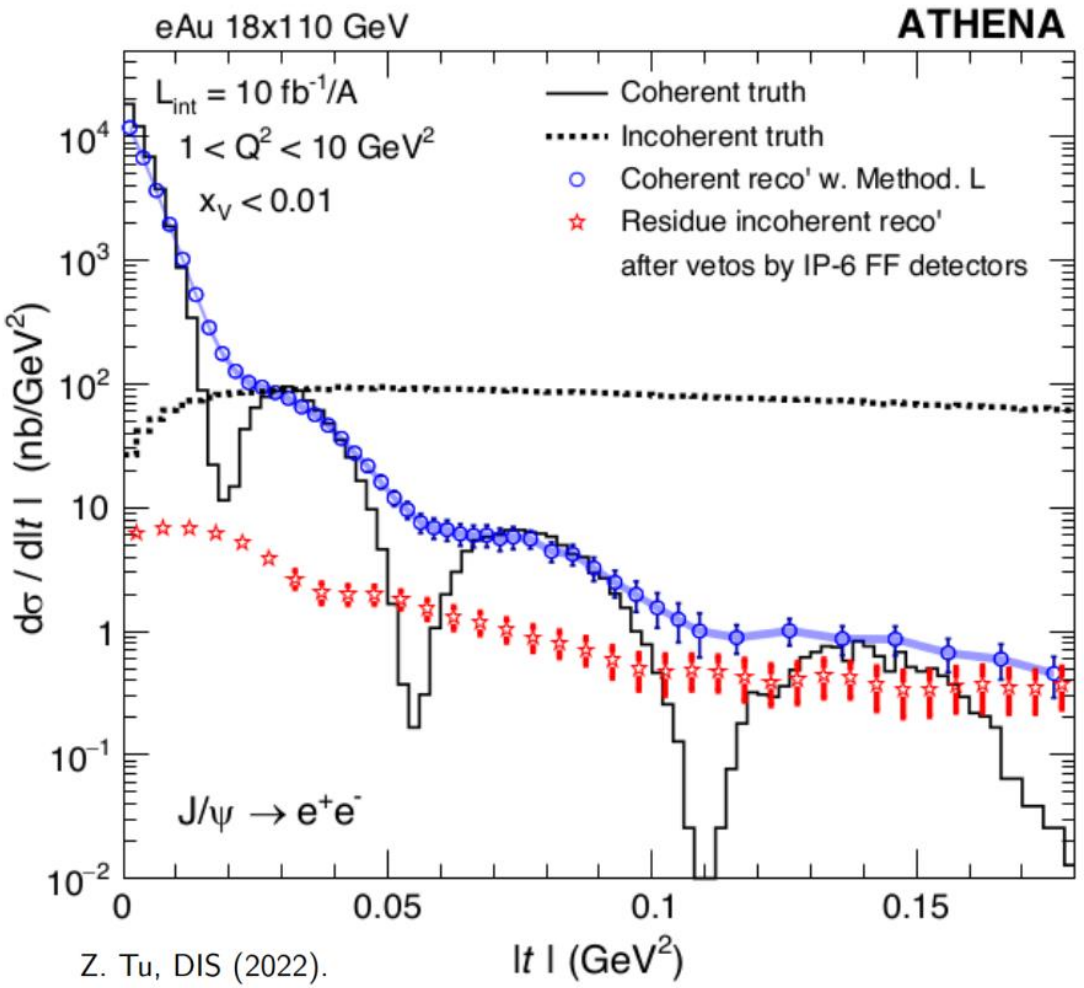

- Exclusive coherent vector meson production on |t| distribution sensitive to the geometry (gluon) distribution at high energy (low-x)
- One of the must-do measurements at EIC
- However, two issues:
  |t| resolution is too bad
  incoherent background too high

What defines coherent diffractive?

Coherent J/ψ in hadronic collisions

- Coherent J/ψ was observed by the ALICE and STAR collaborations

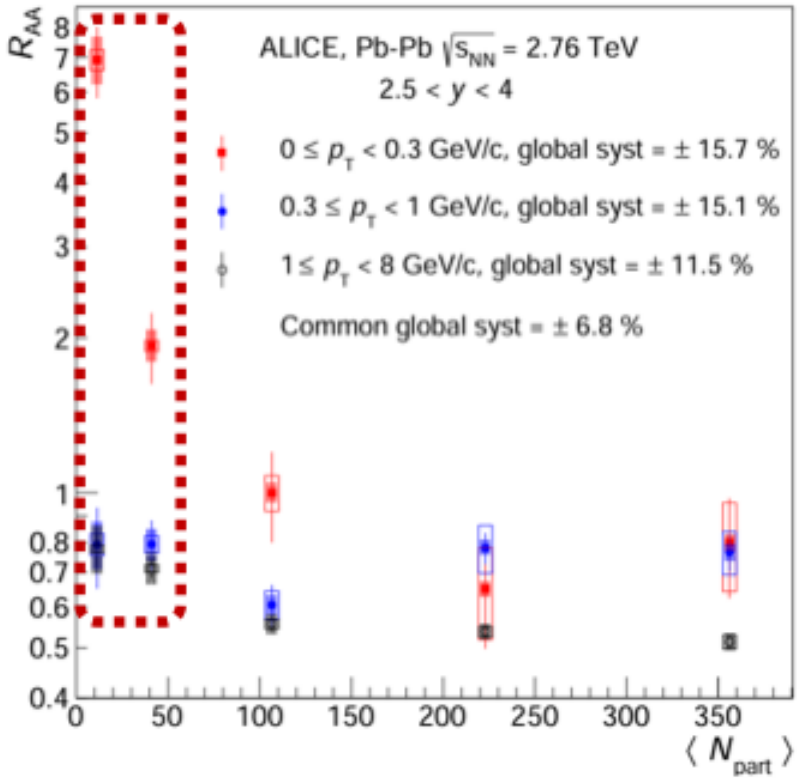

ALICE, Phys.Rev.Lett. 116 (2016) 22, 222301

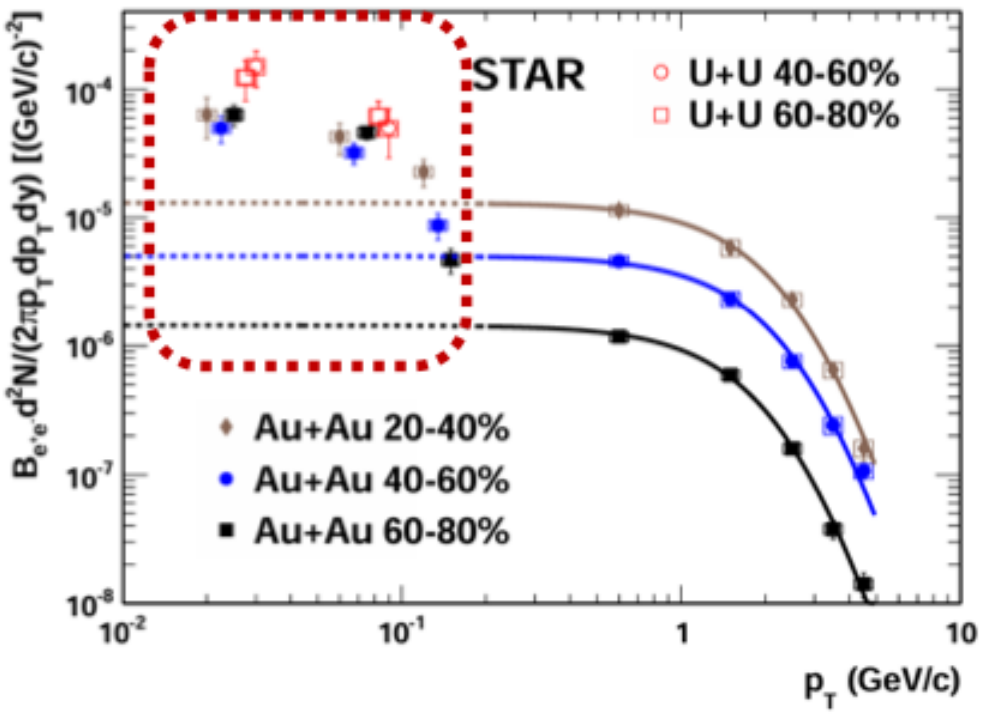

STAR, Phys.Rev.Lett. 123 (2019) 13, 132302

Preserve spin transfer instead of exclusiveness

Cos2Δϕ modulation (A_2) in coherent $J/\psi \to \mu^+\mu^-$

CMS-PAS-HIN-25-006

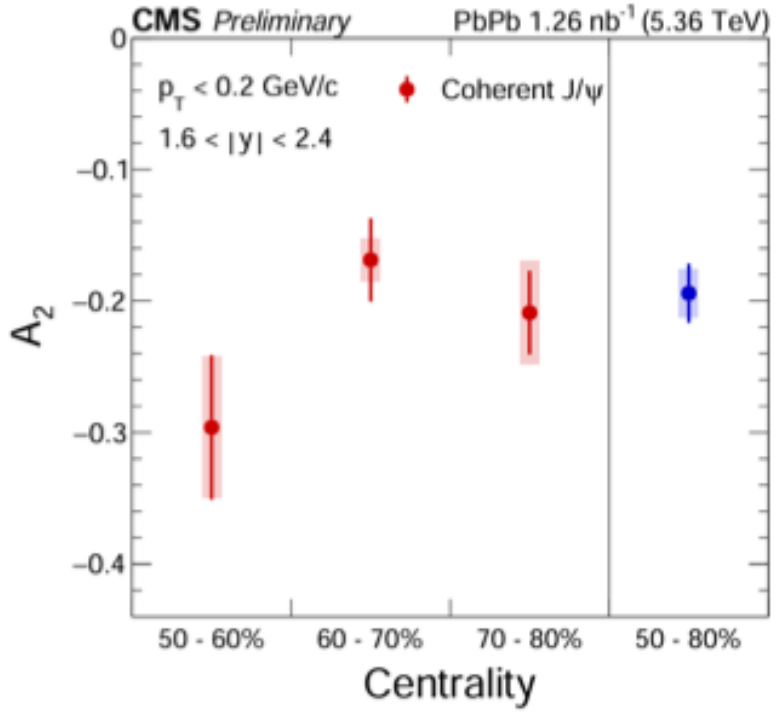

STAR, Sci. Adv. 9 (2023) eabq3903

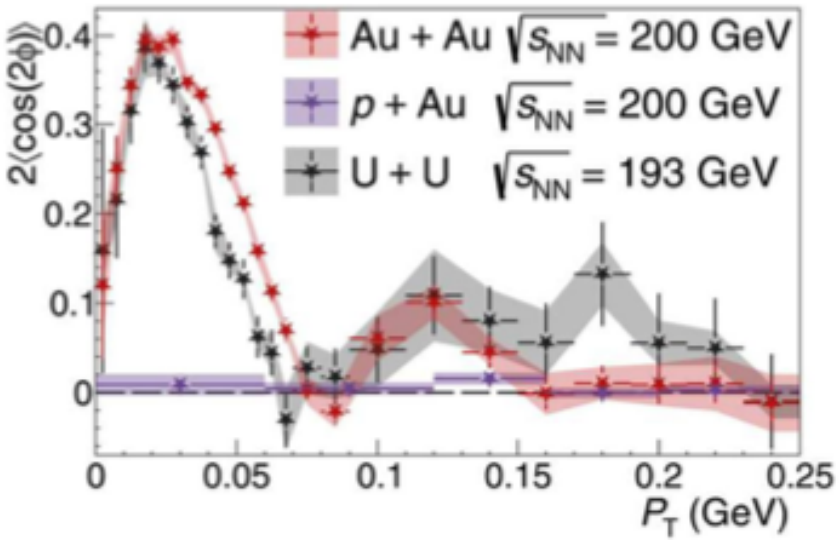

Positive modulation of Coh. $\rho^0 \to \pi^+\pi^-$ (spin-0 bosons) by STAR

- A negative modulation is observed in coherent $J/\psi \to \mu^+\mu^-$ (spin-1/2 fermions) for the first time.
- Together with coherent $\rho^0 \to \pi^+\pi^-$, this provide the first direct observation of the spin-state dependence in coherent VM azimuthal asymmetry.

Spin-based Separation

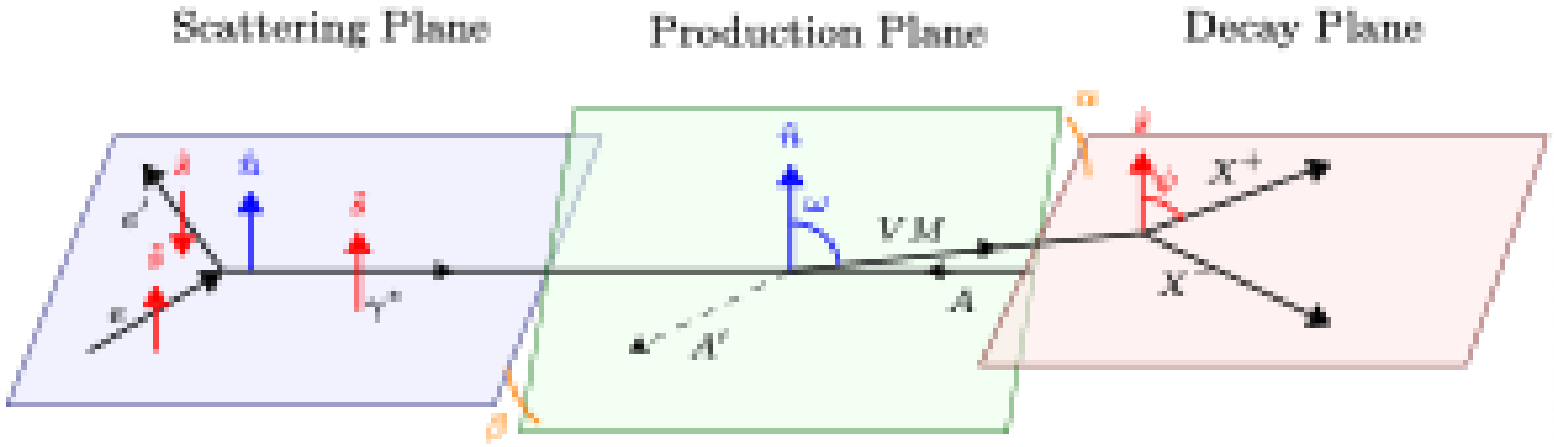

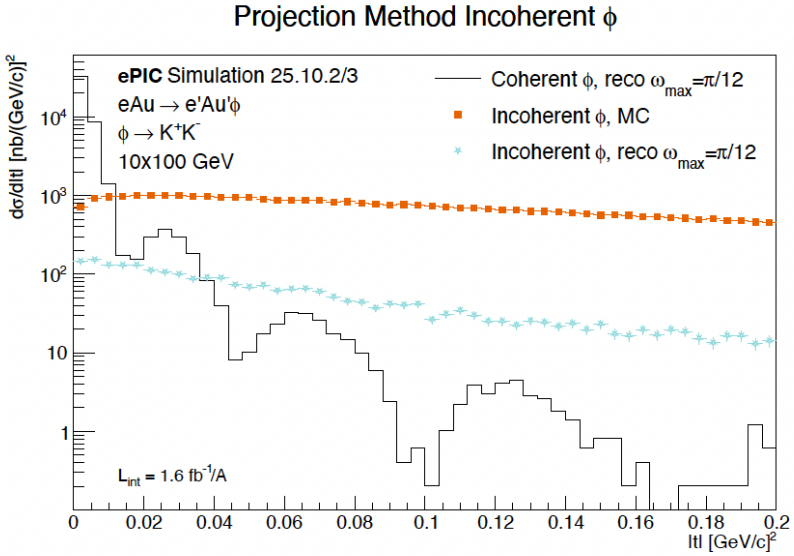

- **Coherent events:**
  - e spin flips: clean spin transfer $e \to \gamma^* \to VM$
    - Observed at HERA arXiv:0910.5831
  - VM's spin direction is fixed
  - Project momentum of VM decay daughter onto VM spin direction → decay shows a $\cos(2\phi)$ modulation
    - Experimentally observed at STAR arxiv:2204.01625
- **Incoherent events:**
  - e spin does not flip → spin transfer is lost
  - VM spin direction random
  - Flat ψ distribution

Summary and Perspectives

- Precise QED calculations and matching experimental data with high statistics from initial photon collisions
- Vector Meson Production with Quantum Entanglement provides very precise mass radius measurement

- Both measurements provide a good constraint on quark and gluon distributions at high energy

- Possible systematical deviation in peripheral at RHIC and central collisions at LHC due to final-state B-field effect
- Model: QED+final-state B-field to match data
- RHIC data with more central collisions and high statistics (2023-2025)
- Derive Pb charge radius from LHC data
- What defines coherent diffractive may be important for EIC and an interesting question by itself
- Projective nuclear imaging is important to measure nuclear geometry at EIC

Pb Mass radius at LHC

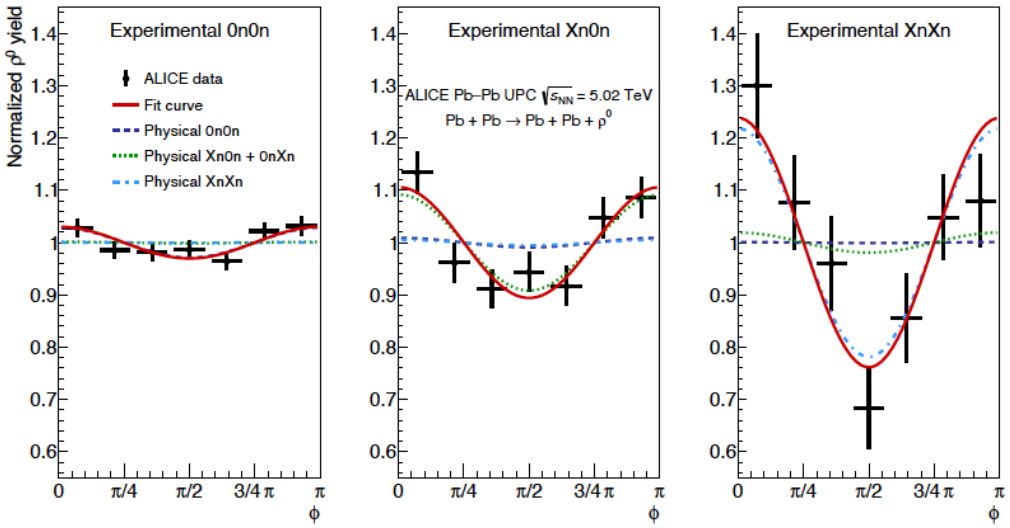

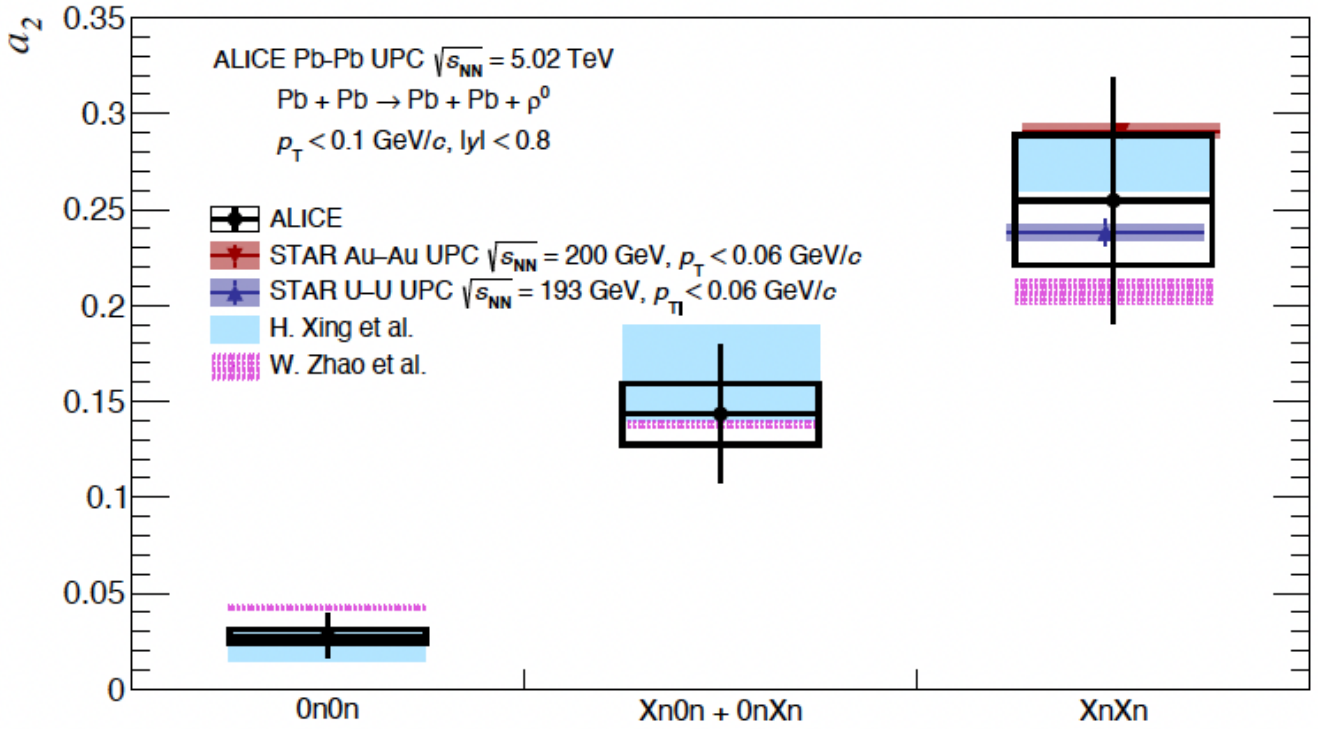

ALICE, *Phys.Lett.B* 858 (2024) 139017

ALICE also observed the rho entanglement effect,
should be able to extract Pb radius with high precision (<1%)

What was used to measure nuclear radii in 1970s?

VOLUME 24, NUMBER 14 PHYSICAL REVIEW LETTERS 6 APRIL 1970

PHOTOPRODUCTION OF NEUTRAL RHO MESONS FROM COMPLEX NUCLEI

H. Alvensleben, U. Becker, William K. Bertram, M. Chen, K. J. Cohen, T. M. Knasel, R. Marshall, D. J. Quinn, M. Rohde, G. H. Sanders, H. Schubel, and Samuel C. C. Ting

Deutsches Elektronen Synchrotron, Hamburg, Germany, and Department of Physics and Laboratory for Nuclear Science, Massachusetts Institute of Technology, Cambridge, Massachusetts 02139

(Received 30 October 1969)

We present results of measurements on photoproduction of ρ mesons. Analysis of 10^6 measured ρ events in a four-dimensional data matrix $d\sigma(A,m,p,t_\perp)/d\Omega dm$ with dimensions $14\times20\times10\times20$ yields precise information on nuclear density distributions for ρ production. We obtain for the Woods-Saxon radii $R(A)=(1.12\pm0.02)A^{1/3}$ and, using the vector dominance model, $\sigma_{\rho N}=26.7\pm2.0$ mb and $\gamma_\rho^2/4\pi=0.57\pm0.10$.

$$\gamma + A \rightarrow A + \rho \quad \rho \rightarrow \pi^+ + \pi^-,$$

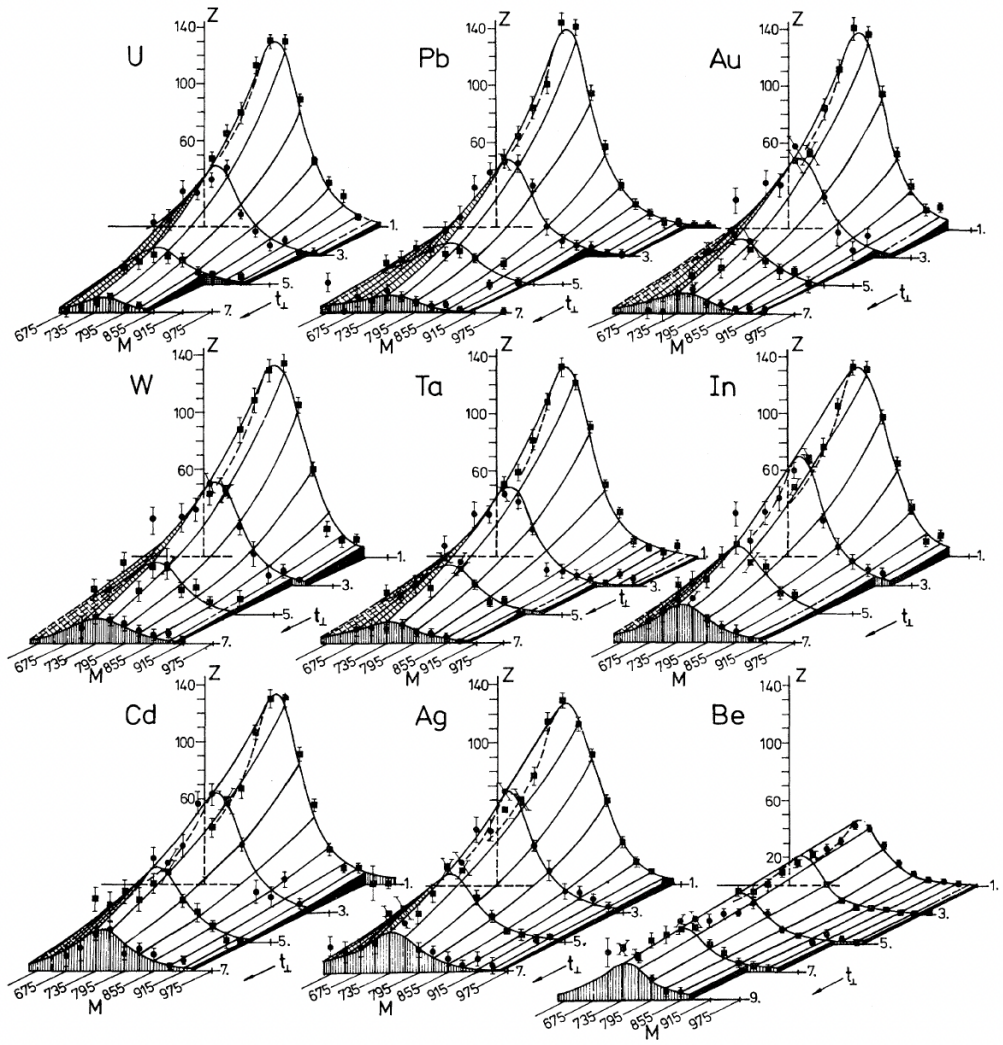

FIG. 1. The cross section $Z=d\sigma/d\Omega dm$ [μb/sr (MeV/c^2) nucleon] as a function of m (MeV/c^2) and $t_\perp$ in units of -0.001 GeV$^2/c^2$ for $p=6.2\pm0.2$ GeV/c. The curves are the best fits to Eq. (2) with $R_1(m)$. The background is not drawn. This figure shows about 2% of the data.

What was used to measure nuclear radii in 1970s?

VOLUME 24, NUMBER 14 PHYSICAL REVIEW LETTERS 6 APRIL 1970

PHOTOPRODUCTION OF NEUTRAL RHO MESONS FROM COMPLEX NUCLEI

H. Alvensleben, U. Becker, William K. Bertram, M. Chen, K. J. Cohen, T. M. Knasel, R. Marshall, D. J. Quinn, M. Rohde, G. H. Sanders, H. Schubel, and Samuel C. C. Ting

Deutsches Elektronen Synchrotron, Hamburg, Germany, and Department of Physics and Laboratory for Nuclear Science, Massachusetts Institute of Technology, Cambridge, Massachusetts 02139

(Received 30 October 1969)

We present results of measurements on photoproduction of ρ mesons. Analysis of 10^6 measured ρ events in a four-dimensional data matrix $d\sigma(A,m,p,t_\perp)/d\Omega dm$ with dimensions $14\times20\times10\times20$ yields precise information on nuclear density distributions for ρ production. We obtain for the Woods-Saxon radii $R(A) = (1.12\pm0.02)A^{1/3}$ and, using the vector dominance model, $\sigma_{\rho N} = 26.7\pm2.0$ mb and $\gamma_\rho{}^2/4\pi = 0.57\pm0.10$.

$$\gamma + A \rightarrow A + \rho \qquad \rho \rightarrow \pi^+ + \pi^-,$$